DESIGN OF HIDAM: HIGHLY DEPLOYABLE ARTICULATED MAST FOR POSITIONING OF SATELLITE COMPONENTS

A Thesis Submitted to
the Graduate School of Engineering and Science of
İzmir Institute of Technology
in Partial Fulfillment of the Requirements for the Degree of

MASTER OF SCIENCE

in Mechanical Engineering

by
Yunus CEBECİ

October 2022
İZMİR

ACKNOWLEDGMENTS

I would like to express my first and foremost gratitude to Dr. Gökhan Kiper, for his invaluable guidance, patience and support during my bachelor's and master's study and especially in this project. His passion, determination and discipline are a model that I will always take as an example for me throughout my life.

Also, I would like to thank to my thesis committee members Dr. Mehmet İsmet Can Dede, Dr. Özgür Kilit and Dr. Gökhan Kiper.

I would like to express my special thanks to Murat Demirel for all the support he has given me as well as the wonderful work he has carried out in the project. At this point, I would also like to thank all the members of the RAML laboratory for all their support.

It is a great accomplishment for me to finish this thesis. This cannot be completed without the indescribable support of İhsan Ruhi Özbek, who will always have a special place for me. He deserves the greatest appreciation.

I express my deepest gratitude to my parents, my brother and sister. Their presence is the most important support in completing this thesis.

This study is funded by 1005 - National New Ideas and New Products Research Funding Program (Ulusal Yeni Fikirler ve Ürünler Araştırma Destek Programı) of The Scientific and Technological Research Council of Turkey (TÜBİTAK) with the project name "Design of Deployable Mast Mechanisms with High Deployment Ratio for Positioning of Satellite Components" and the grant number 120M812. The data and support provided by STM Defense Technologies company is gratefully acknowledged.

ABSTRACT

DESIGN OF HIDAM: HIGHLY DEPLOYABLE ARTICULATED MAST FOR POSITIONING OF SATELLITE COMPONENTS

With the emerging space activities, use of deployable structures for aerospace applications increased in recent years. Deployable masts are special types of these structures where longitudinal deployment is required and deployable truss mast is one of the deployable mast types.

In this thesis, a new design methodology for deployable truss masts is introduced resulting in superior packing ratio. It is a type of a Wren platform which has a single degree of freedom, and it is called HiDAM: Highly Deployable Articulated Mast.

The mathematical model for HiDAM is constructed and the packing ratio is maximized by optimizing part lengths. Considering the set design requirements, the constructional design is carried out, first in two dimensions where mathematical model is developed, then in three dimensions.

Along with the constructional design, the prototype of HiDAM is manufactured and assembled for a single deployable unit with which overall mechanism movement can be seen. It is presented that with the proposed deployable truss mast HiDAM, the packing ratio can be increased by about 12% compared to the most recent deployable truss mast examples in the literature.

ÖZET

UYDU BİLEŞENLERİNİN KONUMLANDIRMASINA YÖNELİK VE YÜKSEK KATLANMA ORANINA SAHİP KATLANABİLİR DİREK MEKANİZMASI TASARIMI

Gelişen uzay faaliyetleri ile son yıllarda uzay uygulamaları için katlanabilir yapıların kullanımı artmıştır. Katlanabilir direkler ise uzunlamasına konuşlandırmanın gerekli olduğu bu yapıların özel tipleridir ve katlanabilir kafes direkler de katlanabilir direkler tiplerinden biridir.

Bu tezde, katlanabilir kafes direkler için halihazırda kullanılan katlanabilir kafes direklerin katlanma oranını artırmak için yeni bir tasarım metodolojisi tanıtılmıştır. Tek serbestlik derecesine sahip bir Wren platformu türü olan bu direk HiDAM: Highly Deployable Articulated Mast (Yüksek Katlanma Oranına Sahip Mafsallı Direk) olarak adlandırılmıştır.

HiDAM için matematiksel model oluşturulmuş ve parça uzunlukları optimize edilerek katlanma oranının artırıldığı gösterilmiştir. Belirlenen tasarım gereksinimleri göz önünde bulundurularak, önce matematiksel modelin geliştirildiği iki boyutlu, ardından üç boyutlu yapı tasarımı yapılmıştır.

Yapısal tasarımın yanı sıra, HiDAM'ın prototipi için, genel mekanizma hareketinin görülebildiği katlanabilir tek modül üretilip montajı gerçekleştirilmiştir. Önerilen katlanabilir kafes direk HiDAM ile, literatürdeki en güncel katlanabilir kafes direk örneklerine kıyasla, katlanma oranının yaklaşık %12 oranında artırılabileceği gösterilmiştir.

TABLE OF CONTENTS

LIST OF FIGURES

Figure **Page**

Figure **Page**

Figure **Page**

LIST OF TABLES

Table **Page**

CHAPTER 1

INTRODUCTION

Aerospace activities have been emerging since 1957 when the USSR launched Sputnik, the first human-made satellite, to orbit Earth. Some of the significant achievements are the completion of the International Space Station (ISS) (Figure 1.1), the Space Shuttle Program, and the most recent achievement is the launching of James Webb Space Telescope in December 2021 (Gardner et al. 2006). The growth in space applications, however, was followed by unconventional engineering problems such as limited cargo volume of spacecrafts to be used to send structures to space. Hence, researchers have been studying to overcome the volume constraint by implementing special mechanisms called deployable structures into the design of space structures.

In this Chapter, a brief overview of deployable space structures is given regarding their effects on astrophysics missions. Also, the scope, aim and outline of the thesis are presented.

Figure 1.1. The International Space Station with its deployable solar panels and other structures (Source: NASA)

1.1. Overview and Design Criteria of Deployable Space Structures

There is a need for structures allowing large volume changes in space since the carrier rockets allow limited cargo volume. There are two types of structures, erectable and deployable structures, that fulfil this request (Mikulas 1993). The former, which can also be called demountable or assemblable structures, requires additional constructional work during the deployment process. This is clearly not practical for space applications as they possess an additional and risky workload for astronauts. Conversely, deployable structures exhibit the possibility of designing the initial and final state of the structure with no additional work. This means that the deployment occurs in accordance with the predetermined design configurations.

Astrophysics missions generally require two types of structures, which can be called one-dimensional and two-dimensional structures. One-dimensional structures, such as deployable masts or booms, are needed when longitudinal (i.e., unilateral) deployment is desired. Deployment of solar panels, the support of payloads away from the main body of a spacecraft and gravity gradient stabilization are some application examples of this type. Two-dimensional structures, on the other hand, are used where the increased aperture is required to enhance angular resolution such as deployable antennas.

As for the design criteria, generally, stowed and deployed (i.e., closed and open, respectively) configurations play an essential role in the design of deployable structures and intermediate configurations are typically not important. First and foremost, the fundamental design criterion is the permissible storage capacity of launch vehicles determined by the dimensions of fairings. The fairing is a part of a spacecraft whose function is to protect payloads against the launching forces such as aerodynamic, thermal and acoustic (NASA 2022) (Figure 1.2).

Other important design parameters include stiffness of the structure both in stowed and deployed mode, actuation system of the deployment, strength and stability of the structure against external forces such as lift-off and orbital forces, material selection considering the weight of the structure and the cost (Kiper and Söylemez 2009).

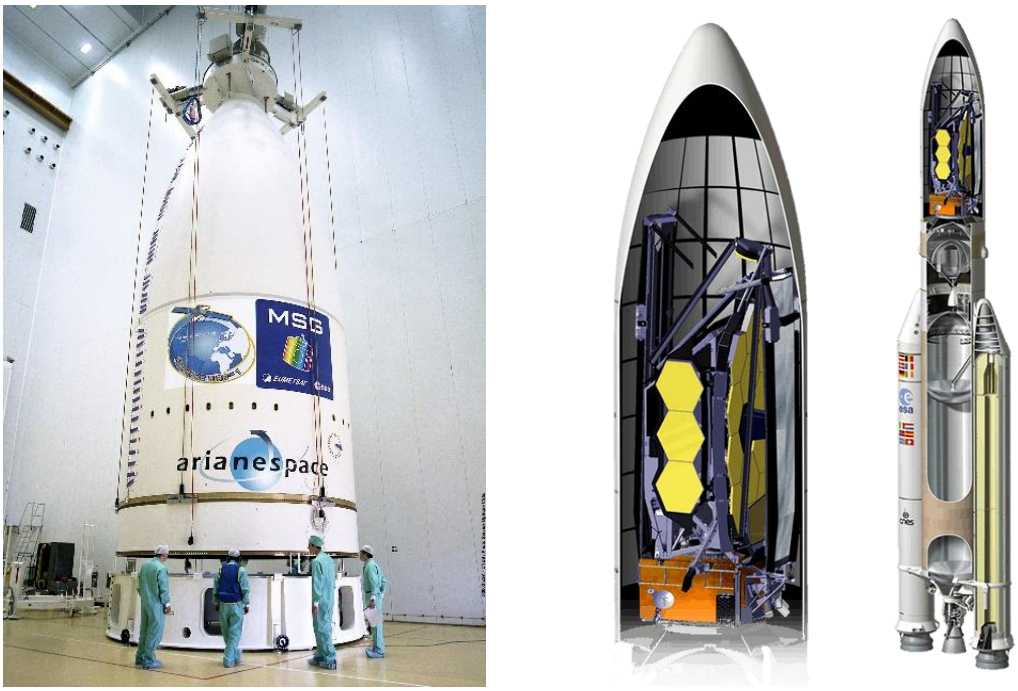

a) b)

Figure 1.2. Some examples of fairings a) The fairing of the MSG-1 satellite at Europe's Spaceport (Source: ESA), b) the fairing of Ariane 5 rocket carrying the James Webb Space Telescope (Source: NASA)

1.2. Motivation of the Thesis

With the technological advances in space applications, there is a trend to substitute large satellites for smaller ones such as CubeSats in low Earth orbit for remote sensing and communications, because these small satellites are now capable enough to perform these applications like conventional large satellites. However, to meet the functionality requirements, they need new design methods for storing and deployment of deployable structures. Consequently, these design alterations created manufacturing problems as well as a reduction in packing ratios owing to the reduced allowable storage capacity (Belvin et al 2016). Hence, improved stowage, deployment characteristics and manufacturability must be considered while designing deployable structures to be used in small satellites.

1.3. Aim of The Thesis

The thesis intends to present a critical review of deployable masts focusing more on deployable truss masts (DTMs) (discussed in Chapter 2) and to propose a deployable mast, namely Highly Deployable Articulated Mast (HiDAM), in which a new constructional design method is developed to maximize the packing ratio. One major issue in the literature is identifying the packing ratio. Another aim of this thesis is to clarify the controversial definition of packing ratio so that it can be used as a fair benchmark.

1.4. Framework of the Thesis

This thesis comprises 5 Chapters. In Chapter 2, the literature survey is given for deployable masts and detailed investigation is presented for deployable truss masts. Later, in Chapter 3, based on the existing deployable truss masts in the literature, the proposed deployable truss mast design is described, the mathematical model and the design of parts are given. In Chapter 4, a prototype of proposed mast HiDAM is presented. Finally, in Chapter 5, the results and conclusions are given.

CHAPTER 2

LITERATURE SURVEY ON DEPLOYABLE MASTS[1]

Deployable mast is a subgroup of deployable space structures. Emerging space activities in recent years have led to the use of these structures in the applications. These structures to be sent to space are, however, limited by the volume of cylindrical payload canisters which are integrated into the cargo bay of space shuttles (Galvez, Gaylor and Young 2011; Puig et al. 2010). Since this volume constraint directly affects the functionality of these structures, it becomes the fundamental design parameter where larger aperture diameters and longer focal lengths are required. To overcome the volume restriction that makes the design of these structures difficult, numerous studies have been published in the past decades. In these publications, researchers mainly focused on improving the packing ratios of these structures, which is the ratio of the design parameter to be measured in the open and closed forms of the structures. For instance, this parameter might be the aperture diameter for deployable antennas and focal length for deployable masts.

There is a large volume of published studies describing the role of deployable mast in the literature. These studies are collected and presented in the past as state-of-the-art by some researchers. One of the first comprehensive reviews on large deployable structures including deployable masts is presented by Pellegrino (1995). Pellegrino focuses on not only deployability but also retractability of structures in this review. Later, Jensen and Pellegrino (2001) extended their reviews and presented the state-of-the-art. Hanaor and Levy (2001) also published a critical review about deployable space structures. This study covers a large volume of references up to that date. Tibert (2002), later on, covered deployable space structures in their doctoral dissertation. There are also some recent review studies on deployable space structures. Kiper and Söylemez (2009)

[1] The main content of this Chapter is presented in Cebeci, Yunus, Murat Demirel, and Gökhan Kiper. 2022. "A Critical Review of Deployable Truss Masts and Proposal of a New Mast: HiDAM." In International Symposium on Unmanned Systems and the Defense Industry (ISUDEF'22), May 30-June 01, 2022. Madrid, Spain and Cebeci, Yunus, Murat Demirel, and Gökhan Kiper. 2021. "Katlanabilir mafsallı kafes direklerin katlanma oranlarını etkileyen faktörlerin incelenmesi ve yeni bir tasarım yönteminin araştırılması." In 20. Ulusal Makina Teorisi Sempozyumu (UMTS 2021), September 15-17, 2021. Diyarbakır, Turkey.

presented a review covering recent advances in space applications. Focusing on deployable structures for astrophysics missions, Puig et al. (2010) introduced a comprehensive review. In their work, they compared the existing structures according to their functionality and trade-off parameters to form a set to be able to choose the best type of structure based on the application.

Several categories have been developed to classify deployable masts in the literature. While Tibert (2002) classifies deployable masts in four groups: thin-walled tubular booms, telescopic masts, coilable masts and articulated trusses, Straubel (2012) prefers to divide deployable masts into three categories as tubes, trusses and other concepts. This thesis reviews only deployable truss masts (DTMs) which are special types of deployable masts that offer appealing solutions for space applications requiring higher payloads, deployment reliability and positioning accuracy (Puig et al. 2010). To make the following parts more understandable and before giving more details about each class, it would be helpful to mention the terminology of DTMs. As represented in Figure 2.1, DTMs involve similar parts generally and the fundamentals are named as such; longerons for longitudinal elements and battens for transverse elements. The longerons and battens may also have hinges at the ends. The boom diameter is represented with R. Additionally, in order to increase stiffness, these structures may also need diagonal cables and latch mechanisms. In this study, the polygonal structures created by battens and longerons are called platforms and legs, respectively.

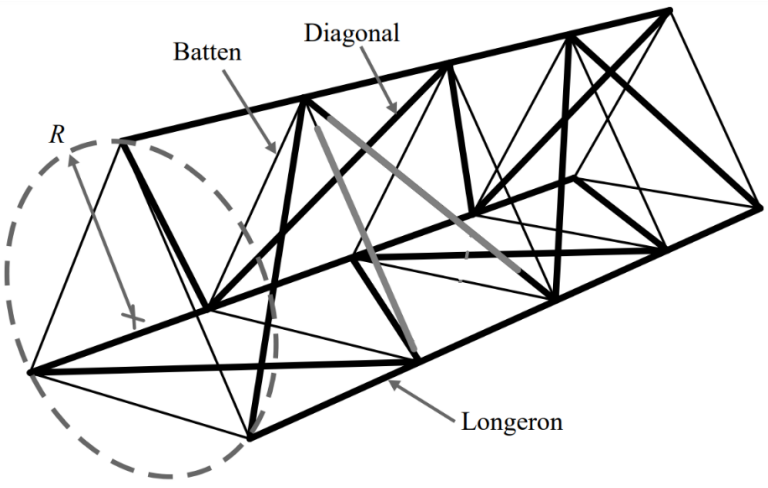

Figure 2.1. Deployable Truss Mast (DTM) terminology (Murphey 2006)

In addition, Pellegrino (2014) describes two folding principles for deployable masts in his book as shown in Figure 2.2, but he did not name each motion type specifically. Based on his description the motions in Figure 2.2 (a) and (b) can be named as translational-type folding and screw-type folding, respectively.

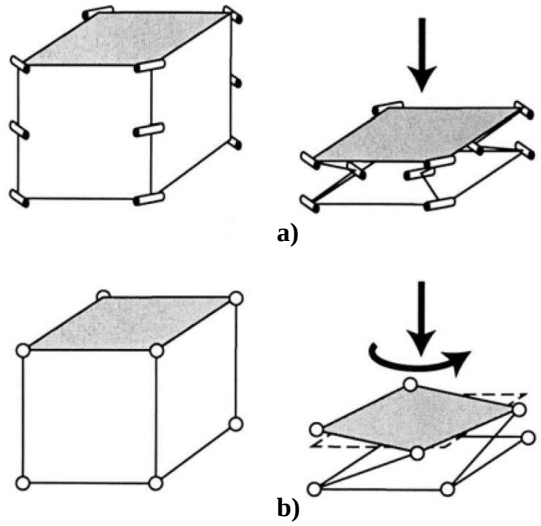

Figure 2.2. Folding Principles, a) translational type, b) screw type (Pellegrino 2014)

It must be stated that these folding principles directly affect the motion of deployable masts realizes. For instance, a mast performs a synchronous deployment if its folding principle is based on the screw type, but if it is the translational type, it executes a sequential deployment.

2.1. Deployable Truss Masts (DTMs): State-of-the-Art

DTM structures generally involve rigid parts compared to other deployable masts/booms solutions such as thin-walled tubular booms. Since DTMs are made up of non-collapsible elements, they need larger canister volumes. However, they are appropriate structures where higher strength and stiffness are required. Moreover, these truss systems have considerable flight heritage in which their reliability and efficiency are proved with several aerospace applications.

The CoilABLE mast design by ATK/ABLE Engineering Company uses continuous longerons, i.e., legs. The method involves coiled members at the most folded form, and it can be deployed with the help of a motor driver or self-deployment is also possible with a method called Lanyard. If actuated with a motor, a cannister-deployed method needs to be used, which results in extra mass. This technology was designed to be used especially in high-precision optics deployment (Figure 2.3 (a) and Figure 2.3 (b)). McEachen (2010) explains in their paper that SAILMAST by ATK/ABLE utilizes this technology, using the strain energy by coiling the longerons to obtain the necessary to deploy these structures. Also, these systems are preferred in space applications as they are lightweight structures.

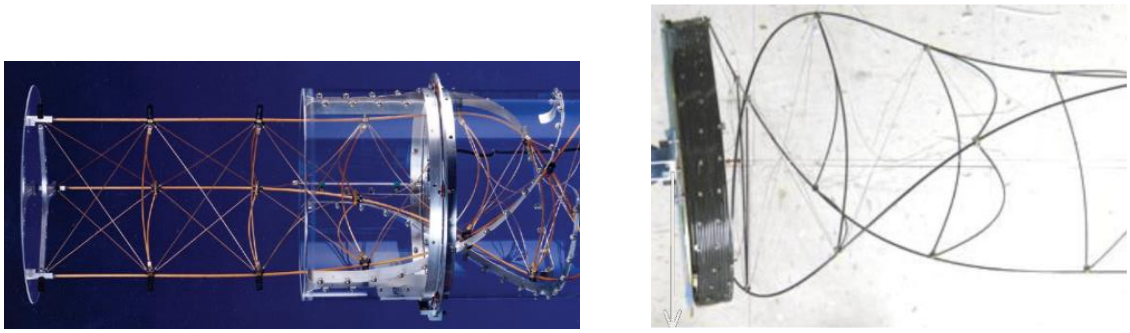

a) b)

Figure 2.3. a) CoilABLE Masts and b) SAILMAST by ATK/ABLE Engineering Company (McEachen 2010)

Although the coilable booms have higher packing ratio and lower masses, if the mission requires higher payloads but also higher deployment reliability and higher positioning accuracy, the articulated masts provide the most appealing solutions. The literature involves some patented articulated masts having a leading role in this field (Benton and Robbins Jr 1986; Hedgepeth and Adams 1986; Kitamura et al. 1990; Mauch 1969). In addition to these pioneering structures, ATK/ABLE Engineering Company designed the Folding Articulated Square Truss (FAST) mast to support the solar arrays on the ISS (Warden 1987) (Figure 2.4 and Figure 2.5). Later, the Able Deployable Articulated Mast (ADAM) was designed as an improved version of the FAST mast and it has been flight proven with many applications such as Shuttle Radar Topography Mission (SRTM) (Figure 2.6) (Gross and Messner 1999; Ramirez 1998). The influence

parameters of the ADAM mast were studied by Xue et al. (2018) in detail as well. Since these masts have longer focal lengths and carry higher payloads, they are mainly used in applications requiring baseline extension with a radar at the tip of the mast or high-resolution optical systems. Additionally, while FAST realizes translational type of folding principle, ADAM has screw type folding principle.

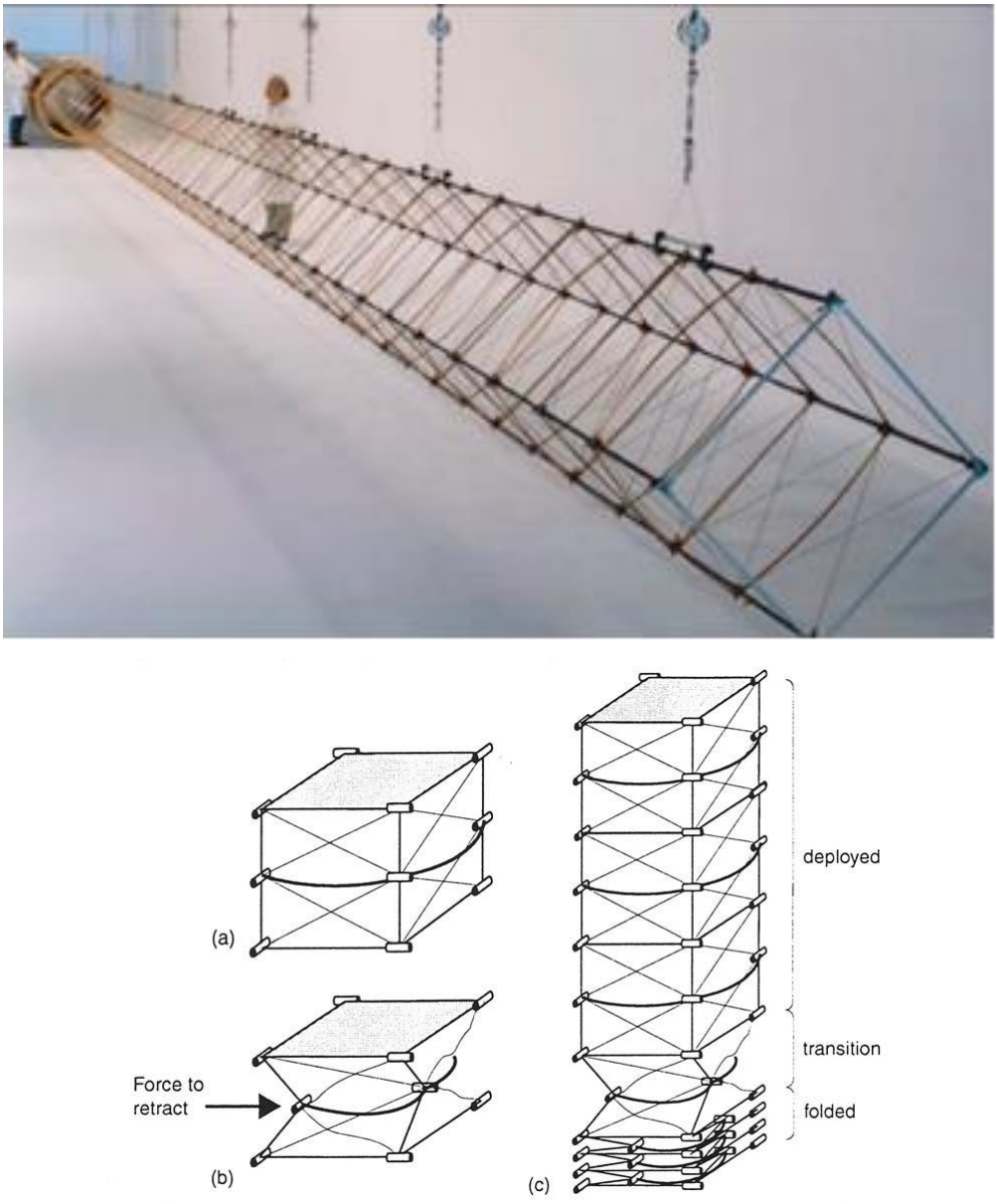

Figure 2.4. FAST Mast used in ISS to support solar arrays and its working principle (Tibert 2002)

Figure 2.5. Solar array wing panels on the International Space Station deployed and supported by the FAST Mast (Source: NASA)

The ADAM mast with the higher thermally stable optical bench and the extra tip adjustment mechanism is used in the Nuclear Spectroscopic Telescope Array (NuSTAR) mission in order to assure that its optics are well-aligned with the detectors. The main assignment of the NuSTAR project was to support X-ray telescopes at the 10 m focal lengths (Kim et al. 2013).

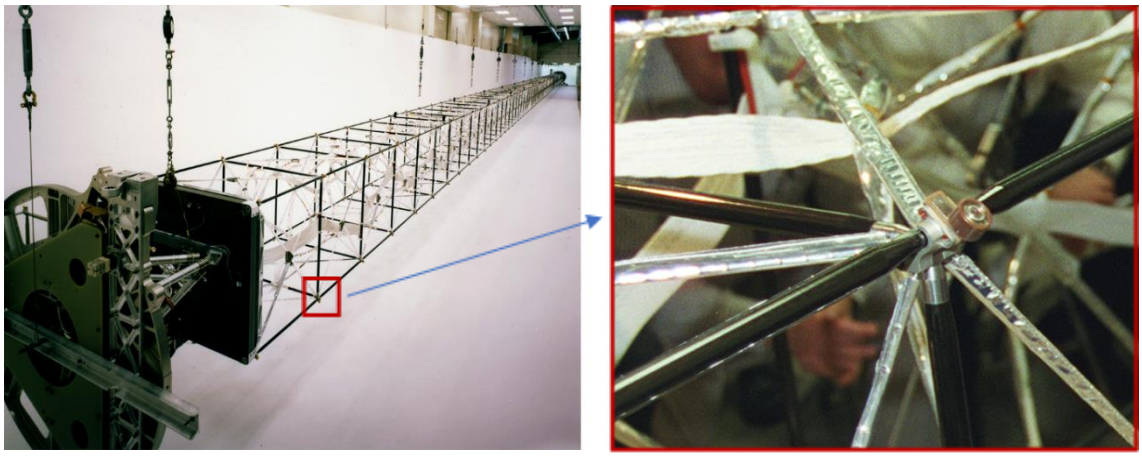

Figure 2.6. ADAM used in SRTM Mission deployed to 60 m with its Hinge Detail View (Ramirez 1998)

Working on the parametric model of the open and closed states of DTMs, Deng et al. (2011) designed a tapered DM with low mass and increased stiffness, for which the height of the DTM can be determined with the given geometrical analysis with no regard to its constructional design (Figure 2.7 (a)). It is shown that the mechanical properties of

the tapered design are improved compared to DTMs with identical cross-sectional areas. Guo and You's (2012) DTM design with serially connected Bennett linkages have single degree-of-freedom (DoF) and its open and closed dimensions can be calculated parametrically (Figure 2.7 (b)). Shan et al. (2013) designed a DTM with a high packing ratio by using triangular prism modules and proved that it is suitable for space applications by studying its kinematics and stiffness (Figure 2.7 (c)). Similarly, Liu et al. (2013) design a DTM in which several octahedrons are connected, and they studied its kinematics along with feasibility (Figure 2.7 (d)). Another novel deployable mast is proposed by Lu et al. (2014) using Hoekens straight-line linkage as a deploying unit and they determined appropriate actuation systems according to static analysis and structural behaviour (Figure 2.7 (e)).

In most space applications, it is desirable to have a constant orientation of the tip of the mast during the motion. For instance, deploying the solar panels of the ISS requires only translational motion and most of the components to be located at a distance out of the satellite body such as cameras and sensors should not rotate during deployment. To achieve this, researchers made use of a Borel-Bricard motion (Bricard 1896; Borel 1905). It is a spatial motion in which all point paths are spherical curves. It is used in the design of a DTM based on Wren platforms by Kiper and Söylemez (2011), where over-constrained single-DoF mechanisms with Borel-Bricard motion are investigated (Figure 2.7 (f)). Lee and Herve (2014) also studied mechanical realizations of the Borel-Bricard motion in detail.

Based on the work by Kiper and Söylemez (2011), Zhao et al. (2018) proposed a DTM system, which has better stiffness characteristics than ADAM. They designed and made a prototype of the Self-Lockable Deployable Structure (SDS) which comprises a reconfigurable extended joint (REJ). This DTM was patented by Wang et al. (2016). This unit also realizes Borel-Bricard motion. Once the mast is fully deployed, a singularity occurs due to the self-motion of the legs. As a result, it becomes self-locked against longitudinal forces. When the mast is fully deployed, only the first two units need to be folded to lock the entire structure completely. Figure 2.8 shows the SDS and its configurations. Here, the hinges used to connect the legs and platforms at the corners are called H-joint which have 3-DoF with 2 parallel axes and an axis perpendicular to them.

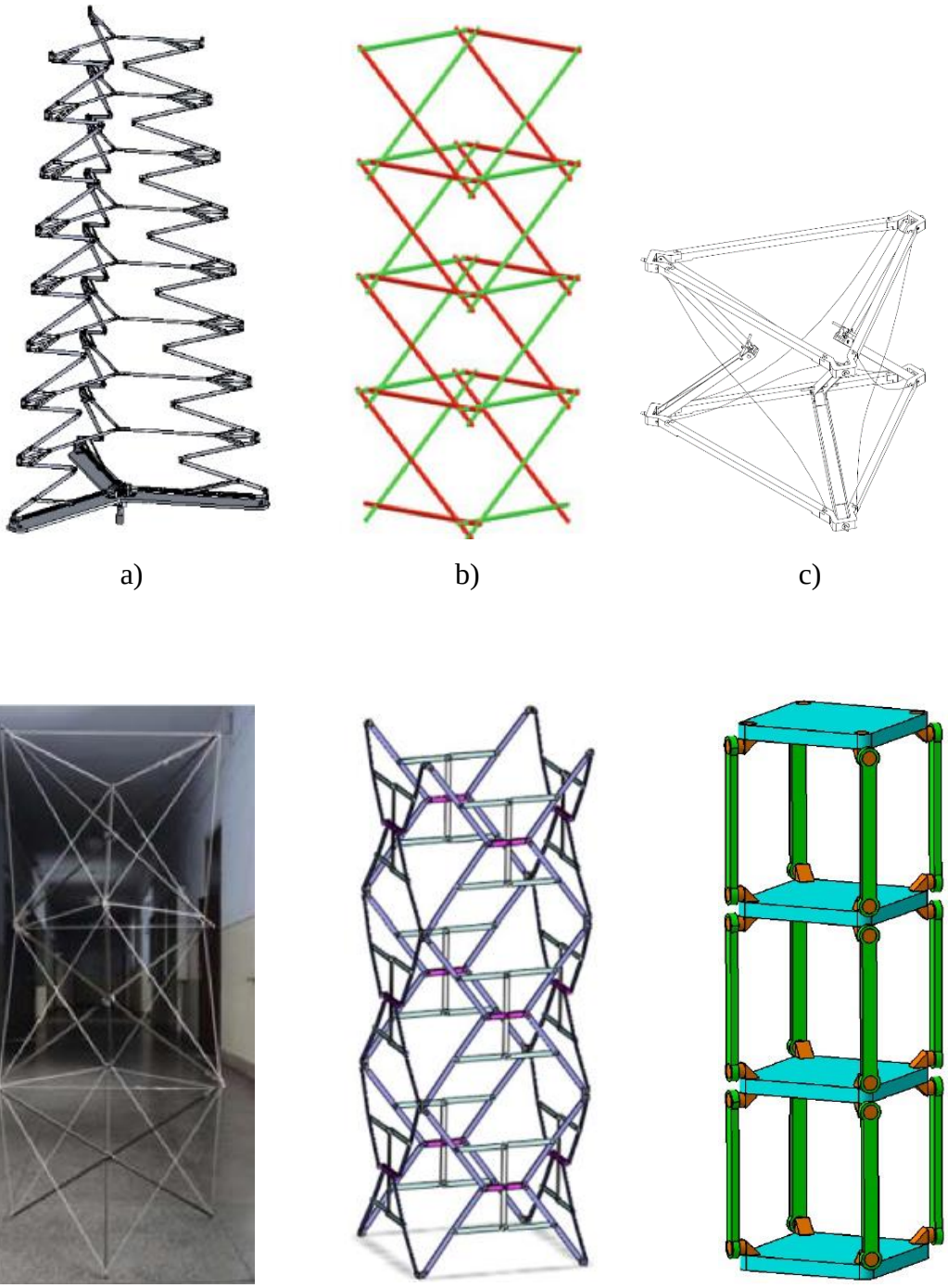

a) b) c)

d) e) f)

Figure 2.7. Recent DTMs in the literature a) Tapered deployable mast (Deng et al. 2011), b) Deployable mast based on Bennett Linkage (Guo and You 2012), c) Triangular prism modular deployable mast (Shan et al. 2013), d) Octahedron deployable mast (Liu et al. 2013), e) Deployable mast based on Hoekens linkage (Lu et al. 2014), f) A deployable mast with square polygonal links (Kiper and Söylemez 2011)

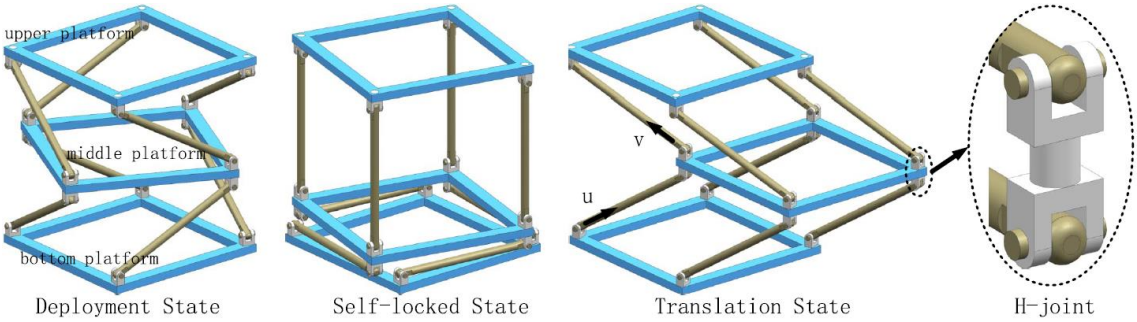

Figure 2.8. Self-Lockable Deployable Structure (SDS) (Zhao et al. 2018)

Another DTM based on Wren platforms is proposed by Wang et al. (2022) recently, in which the link lengths are optimized to maximize the packing ratio by replacing universal joints with a pair of skew revolute joints. In other words, the H-joint in SDS is altered by adding an offset. This additional offset feature is independently invented by Kiper, Demirel and Cebeci (2019). They also developed a mathematical model and proved that this DM has the largest packing ratio of all comparable structures in the literature (Figure 2.9). By examining these DTMs, it is seen that the packing ratio can be increased by modifying constructional details. In the next section, a new DTM called Highly Deployable Articulated Mast (HiDAM) is introduced and compared with the other DTMs in the literature.

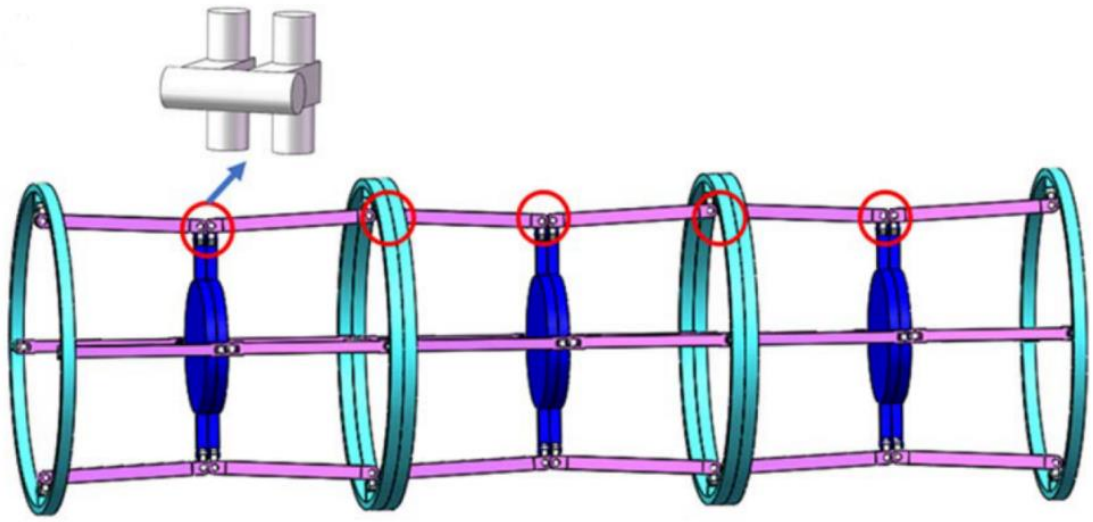

Figure 2.9. The proposed DTM based on Wren Platforms by Wang et al. (2022)

The most recent example of DTM structures is published by Sun et al. (2022). They made use of the motion characteristics of the four-bar slider-crank mechanism to develop a DTM with a constant cross-section with single DoF (Figure 2.10). To attain the deployment of units they implemented gear mechanisms at the corners.

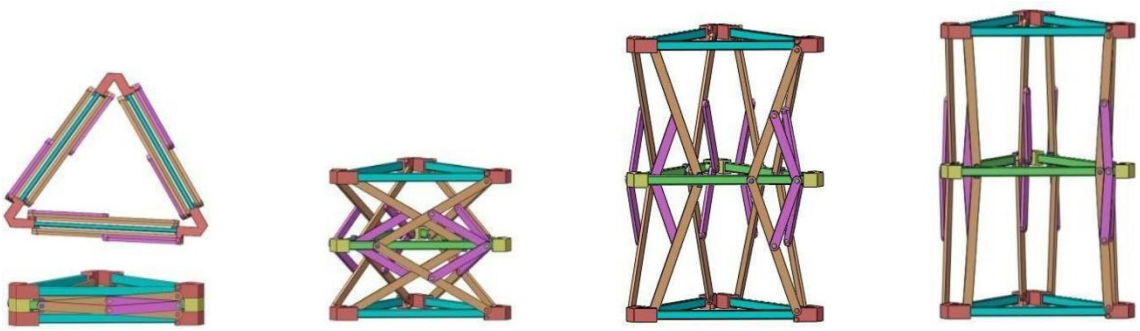

Figure 2.10. The DTM based on four-bar slider-crank mechanism with gears at the corners proposed by Sun et al. (2022)

CHAPTER 3

DESIGN OF THE PROPOSED DEPLOYABLE MAST: HIDAM

In this Chapter, a new highly deployable articulated mast, HiDAM, is introduced. First, the design requirements and brief information about the need for Wren platforms are given. Then, the most recent DTM structures previously mentioned in Chapter 2.1 proposed by Zhao et al. (2018) and Wang et al. (2022) are investigated. Later, the proposed improvements are demonstrated, and the design of the parts is given along with the selection of materials.

3.1. Design Requirements for HiDAM

The design project of HiDAM is funded by 1005 - National New Ideas and New Products Research Funding Program of The Scientific and Technological Research Council of Turkey (TÜBİTAK). The design requirements for this project are specified by STM Defense Technologies company, which are

- **Mast diameter:** 90 mm
- **Maximum stowage height:** 55 mm
- **Maximum Mass:** 200 gr
- **Three-axis sinusoidal vibration:** 5-100 Hz, 4.5g
- **Three-axis static load:** 8.75g
- **Stiffness:** minimum 150 Hz at stowage

The company suggested some design methods based on previous applications under the mentioned mechanical loads. According to that, revolute joints should be used in mechanism, torsion springs can be used for actuation, materials for structural parts should be aluminum, springs and connectors should be steel and coating should be preferred where aluminum and steel are used together.

3.2. The Need for Wren Platforms for Space Applications

Some aerospace applications require a mast with a tip which has a constant orientation. For instance, if the mast is used to deploy solar arrays or antenna membranes, there must only be a translational deployment in one direction, but no rotation. The previously mentioned CoilABLE and SAILMAST, however, have a rotating tip as they are coiled for storage. Hence, researchers made use of some existing mechanisms that inherently provide non-rotating moving platforms. Moreover, to facilitate the deployment process and avoid additional costs, it is preferred that the designed masts have single DoF. The Wren platform, which is a special nSS (S: spherical joint) or nUU (U: universal joint) parallel mechanism realizing the Borel-Bricard motion, attracted scientists to adopt it in the design of deployable masts to fulfil these requirements.

3.3. Investigation of Recent DTM Structures

Before starting the design of HiDAM, similar DTMs realizing Borel-Bricard motion were examined. Kiper and Söylemez (2011) came up with a modified Wren platform which can be used as a deployable mast. It is shown that the spherical joints can be replaced with U joints and finally they proposed a DTM by serially connecting 3-UU parallel manipulators. The working principle of the systems described in the paper is screw-type folding, which is achieved by joining identical legs with universal joints to platforms of equal or similar polygonal shapes. However, in their study, the modules formed by connecting both ends of the 4 legs to the square platforms with the universal joints move freely. Considering this platform type, this project aims to design a DTM with each module moving at the same time, the end platform only realizing a translational motion, and a higher packing ratio compared to those in the literature.

In the literature, the DTM example developed for this purpose is encountered in the structure designed by Zhao et al. (2018). They introduced a component called H-joint represented in Figure 3.1 to obtain a synchronous deployment of all units. However, it has been seen that the packing ratio of this structure can be increased by designing the hubs (connecting elements at the corners) with an offset.

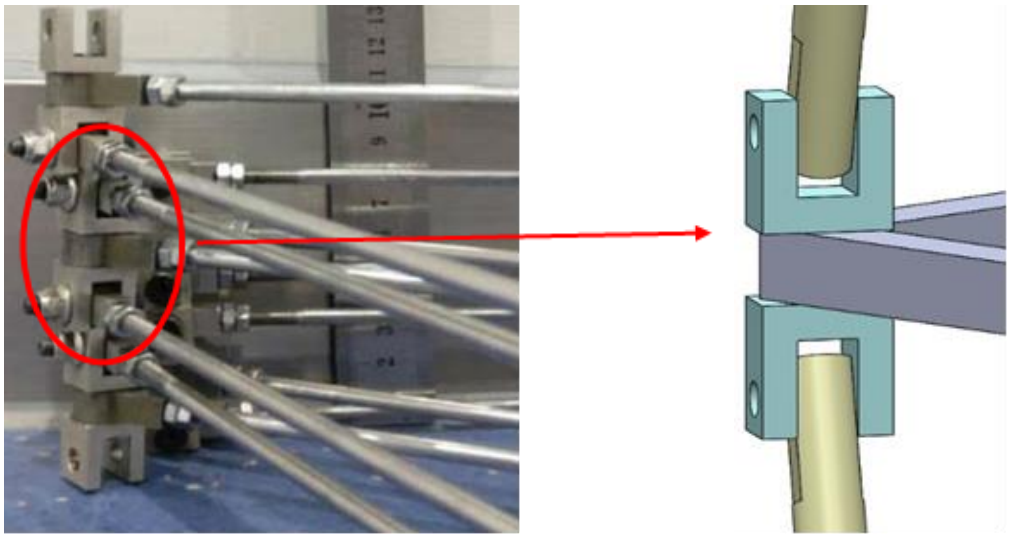

a) b)

Figure 3.1. The H-joint designed by Zhao et al. (2018) a) the manufactured part, b) the 3D CAD model

To illustrate, the centers of the universal joints are designed so that they are no longer intersecting yet have a certain distance. It is seen that the legs can be joined to hubs with less height required. This idea has been studied by Wang et al. (2022) recently and they proposed a DTM where they altered the hub element by adding an offset. With the help of this modification, they were able to place the platform in a flat form and design the platforms to act as the perimeter boundary to avoid overlaps within the allowable volume. Although this design makes it easier to position the parts, it also causes a loss of usable circumference due to the platform wall thickness, so it causes using shorter legs which adversely affect the packing ratio as seen in Figure 3.2.

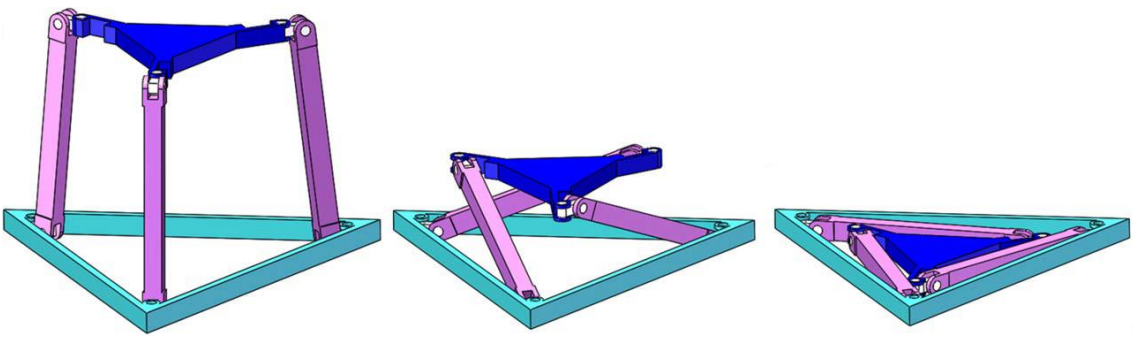

Figure 3.2. The flat foldable DTM proposed by Wang et al. (2022)

3.4. Mechanism Design of HiDAM

The part with offset is compared with the H-joint in Figure 3.3. While the connection and hub dimensions determine the stowage height of a DTM, the most important dimension for the open height is the longeron lengths. Therefore, the longest longeron length that can be positioned in a circle, which does not affect the folding of the structure and in the closed state, where overlaps are minimized, should be aimed. In the closed height of DTM design by Zhao et al. (2018), it is seen that the leg lengths are shortened to prevent joint conflicts at the corners. Although this helps to reduce the closed state height, the effect of increasing the folding ratio is not significant since it also reduces the open height of the structure. Considering a structure in which both the leg length is increased, and the corner hubs are prevented from colliding, it has been seen that instead of using the H-joint, designing the joints that are perpendicular to the parallel joints with an offset can allow this (Figure 3.3). Wang et al. (2022) also used a joint structure with eccentricity as mentioned before. In addition, the different platform sizes also increase the folding rate in their study. Although the idea of the kinematic model that will be proposed is similar to the study of Wang et al. (2022), a new constructional design has been presented, which results in a higher packing ratio for similar design criteria.

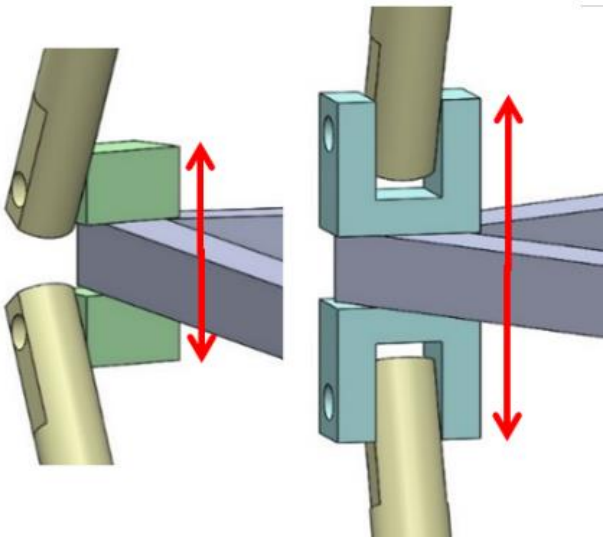

a) b)

Figure 3.3. Comparison of the hub elements a) the hub element of the proposed design, b) the hub element called H-joint (Zhao et al. 2018)

Another aim of this thesis is to create a mathematical model of HiDAM that includes not only part size constraints but also part cross-section thicknesses. To achieve this, several layout trials have been studied. First, models consisting of different or equivalent platforms with triangular star geometry were studied. It is because of the fact that compared to the platform type that is used as an outer boundary in Wang et al.'s DTM which causes using of shorter legs, proposing a triangular platform whose diameter is smaller than the permissible diameter allows using longer legs in the same diameter constraint. The number of platform sides can be chosen as desired, but maximum leg length is obtained with the triangular platform. Planar projections of two of the studied models are given in Figure 3.4. The aim of working with planar projections is to determine the longest leg length in a circle of a certain diameter by creating a mathematical model that can be optimized for closed leg overlaps and includes leg dimensions. For the determination of the kinematic dimensions of the mechanism, kinematic equations alone are not sufficient, the constructional design in 2 dimensions (2D), that is, the section thickness of the legs should also be considered.

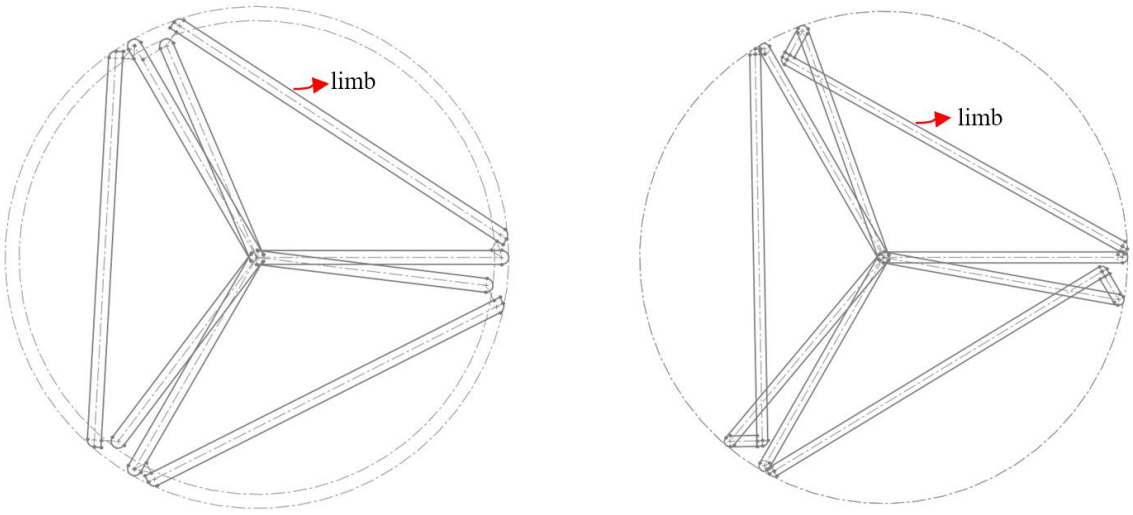

a) b)

Figure 3.4. The layout of the model consists of platforms of a) different diameters, b) equal diameters

In both models in Figure 3.4, the radius of one or both platforms are equal to the radius of the cylindrical volume in which the HiDAM must be placed. It has been seen that different solutions can be obtained in cases where the offset of the hubs at both ends

of a leg is on the same or different sides. In addition, the legs can be placed in the projection plane in such a way that they do not overlap with the platform, as in Figure 3.4 (a), or in such a way that they overlap as in Figure 3.4 (b). Different geometric constraint equations can be obtained according to which parts contact the outer boundary circle whose diameter is 90 mm in our case.

3.5. Mathematical and Optimization Model of HiDAM

As a result of several layout trials similar to the ones in Figure 3.4, the final layout of parts' location is decided as seen in Figure 3.5. It is seen that it is crucial to decide on the design constructions as they affect how the parts are efficiently located in an allowable circle.

Figure 3.5 shows the top view of a triangular mast in its compact form. First, joints of concern are enumerated by i = 0, 1, …, 7. $\mathbf{S_i}$ is the unit vector along joint i, $\mathbf{A_{ij}}$ is the unit vector along the common normal between joint axes i and j = i + 1 (directed from i to j), O_i is on $\mathbf{S_i}$, P_j is the intersection point of $\mathbf{A_{ij}}$ and $\mathbf{S_j}$, a_{ij} is the distance of the common normal between $\mathbf{S_i}$ and $\mathbf{S_j}$, d_i is the directed distance between $\mathbf{O_i}$ and $\mathbf{P_i}$ according to Denavit-Hartenberg (DH) convention (Denavit and Hartenber 1955). We adopt the DH notation as explained by McCarthy (2010) which is represented in Figure 3.6. The design parameters are listed in Table 1. Some of the parameters were taken as pre-selected values according to the design criteria, while others were taken as the variables to be determined as optimum for the maximum value of the leg length in accordance with the kinematic constraints.

Based on the schematic illustration in Figure 3.5, the conditions for the layout of the mast in its stowed form are formulized in order to have a mathematical model to be used to optimize the packing ratio of the deployable mast.

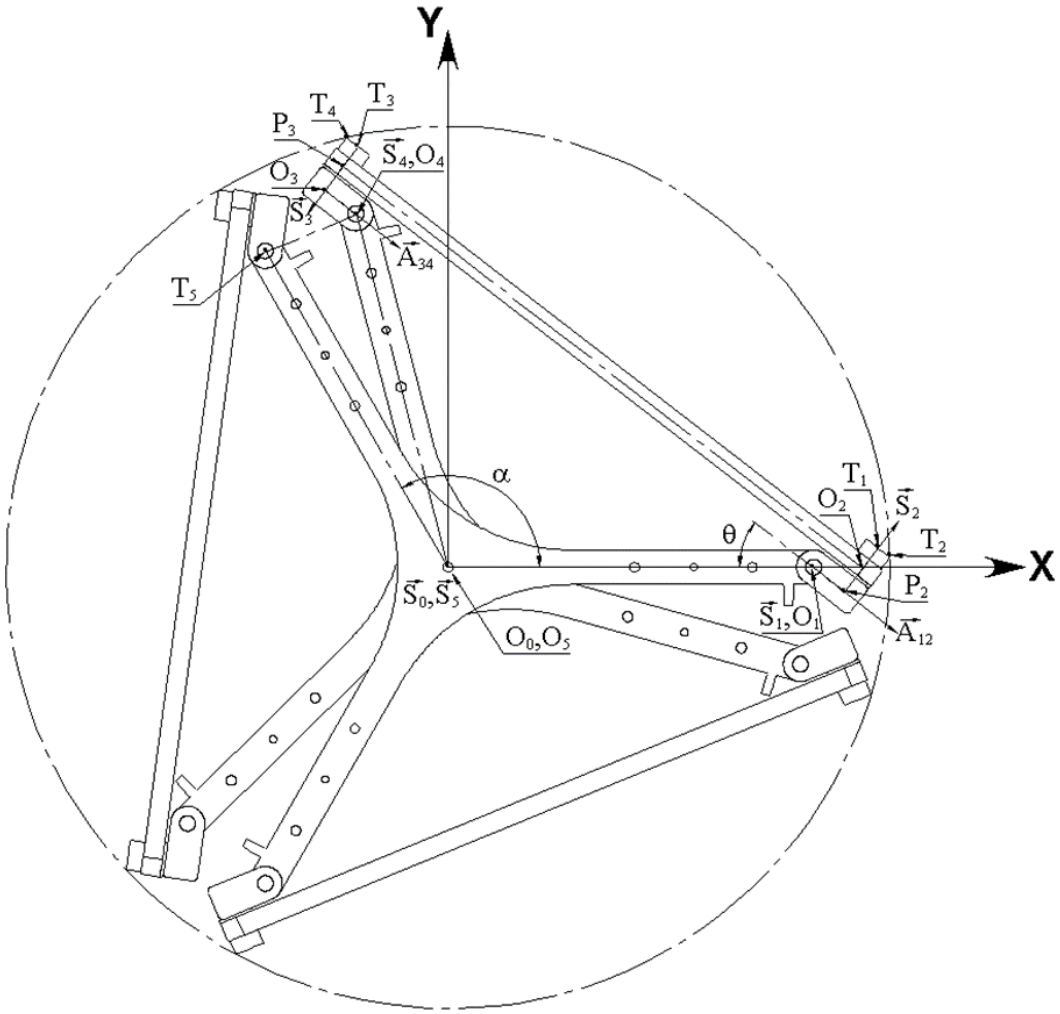

Figure 3.5. The top view of a triangular mast in its compact form to be used to generate its mathematical model comprising necessary vectors

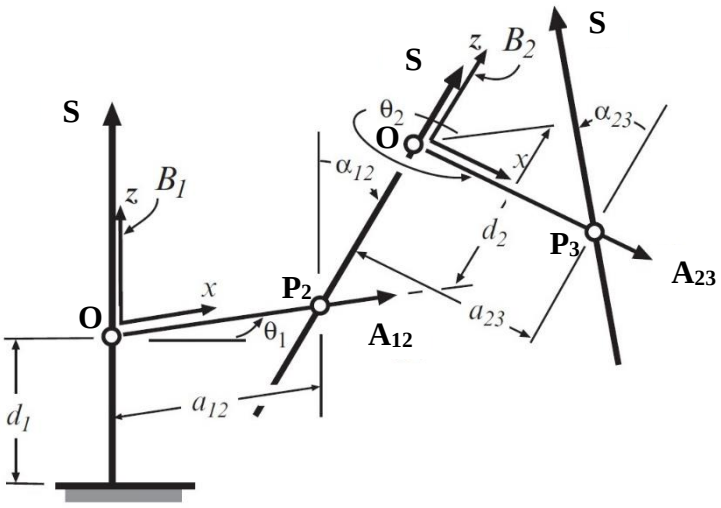

Figure 3.6. DH notation adopted from (McCarthy, 2010)

Table 3.1. Design Parameters of HiDAM

	Parameters	Defined / Free	Selected Value
$\angle O_1O_0T_5$	α	defined	120°
$\lvert O_0O_1 \rvert$	a_{01}	free	-
$\lvert O_1P_2 \rvert$	a_{12}	defined	4.00 mm
$\lvert P_2O_2 \rvert$	d_2	defined	3.05 mm
$\lvert O_2P_3 \rvert$	a_{23}	free	-
$\lvert P_3O_3 \rvert$	d_3	defined	3.05 mm
$\lvert O_3O_4 \rvert$	a_{34}	defined	4.00 mm
$\lvert O_4O_5 \rvert$	a_{45}	free	-
$\lvert O_2T_1 \rvert$	t_1	defined	2.50 mm
$\lvert T_1T_2 \rvert$	t_2	defined	1.50 mm
$\lvert P_3T_3 \rvert$	t_3	defined	2.50 mm
$\lvert T_3T_4 \rvert$	t_4	defined	1.50 mm
$\lvert O_4T_5 \rvert$	t_5	defined	10.00 mm
	r	defined	45 mm
	θ	free	-

Firstly, using the loop closure equation for the loop $O_0O_1P_2O_2P_3O_3O_4O_5$

$$
\begin{aligned}
a_{45}{}^2 &= \left|\overrightarrow{O_5O_4}\right|^2 = \left|\overrightarrow{O_0O_1} + \overrightarrow{O_1P_2} + \overrightarrow{P_2O_2} + \overrightarrow{O_2P_3} + \overrightarrow{P_3O_3} + \overrightarrow{O_3O_4}\right|^2 \\
&= \left(a_{01} + a_{12}c\theta + d_2s\theta - a_{23}c\theta - d_3s\theta + a_{34}c\theta\right)^2 + \left(-a_{12}s\theta + d_2c\theta + a_{23}s\theta - d_3c\theta - a_{34}s\theta\right)^2 \quad (3.1) \\
&= \left[\left(a_{01} + \left(a_{12} - a_{23} + a_{34}\right)c\theta + \left(d_2 - d_3\right)s\theta\right)\right]^2 + \left[\left(d_2 - d_3\right)c\theta + \left(a_{23} - a_{12} - a_{34}\right)s\theta\right]^2
\end{aligned}
$$

where c and s are abbreviations of cosine and sine, respectively. Secondly, point T_2 must be on the outer circle, which is formulized as

$$\begin{aligned} r^2 &= \left|\overrightarrow{O_0O_1} + \overrightarrow{O_1P_2} + \overrightarrow{P_2T_1} + \overrightarrow{T_1T_2}\right|^2 \\ &= \left[a_{01} + (a_{12} + t_2)c\theta + (d_2 + t_1)s\theta\right]^2 + \left[-(a_{12} + t_2)s\theta + (d_2 + t_1)c\theta\right]^2 \end{aligned} \tag{3.2}$$

For the third condition which is similar to the previous one, point T_4 must be on the outer circle:

$$\begin{aligned} r^2 &= \left|\overrightarrow{O_0O_1} + \overrightarrow{O_1P_2} + \overrightarrow{P_2O_2} + \overrightarrow{O_2P_3} + \overrightarrow{P_3T_3} + \overrightarrow{T_3T_4}\right|^2 \\ &= \left[a_{01} + (a_{12} - a_{23} - t_4)c\theta + (d_2 + t_3)s\theta\right]^2 + \left[(d_2 + t_3)c\theta + (a_{23} - a_{12} + t_4)s\theta\right]^2 \end{aligned} \tag{3.3}$$

For the last condition, we have a minimum approaching distance constraint to prevent interference between the corner parts, which is defined as t_5 between O_4 and T_5:

$$t_5^{\,2} = a_{45}^{\,2} + a_{01}^{\,2} - 2a_{45}a_{01}c\left\{\alpha - \operatorname{acos}\left[\frac{a_{01}^{\,2} + a_{45}^{\,2} - (a_{23} - a_{12} - a_{34})^2}{2a_{45}a_{01}}\right]\right\} \tag{3.4}$$

As listed in Table 1, among 15 parameters, definitely given parameters are a_{12}, d_2, d_3, a_{34}, t_1, t_2, t_3, t_4, t_5 and r, and free parameters are a_{01}, a_{23}, a_{45} and θ. Since the goal is to maximize the deployed height of the mast, the optimization problem is to determine free parameters a_{01}, a_{23}, a_{45} and θ such that a_{23}, which represents the distance between the leg's revolute joints, is maximum subject to Equations (3.1), (3.2) and (3.3). Equation (3.4) will then be used to define t_5 as a function of a_{01}, a_{23} and a_{45}. There is also an inequality constraint for θ such that $\theta > 30°$ to avoid configuration change in which interference occurs between parts. Also, in order for the standardization of the parts, the following parameters are chosen to be equal to each other:

$$a_{01} = a_{45},\ a_{12} = a_{34},\ d_2 = d_3,\ t_1 = t_3$$

Firstly, we arrange Equation (3.2) to leave a_{01} alone, which is in terms of θ only:

$$a_{01} = \sqrt{r^2 - \left[(d_2 + t_1)c\theta - (a_{12} + t_2)s\theta\right]^2} - (a_{12} + t_2)c\theta - (d_2 + t_1)s\theta \tag{3.5}$$

If we leave a_{23} alone in Equation (3.3), it will be in terms of θ only.

$$\begin{gathered}\left(a_{12}-a_{23}-t_4\right)^2+2a_{01}c\theta\left(a_{12}-a_{23}-t_4\right)=r^2-{a_{01}}^2-\left(d_2+t_3\right)^2-2a_{01}\left(d_2+t_3\right)s\theta \\ \Rightarrow a_{23}=a_{12}-t_4+a_{01}c\theta\pm\sqrt{r^2-\left(a_{01}s\theta+d_2+t_3\right)^2}\end{gathered} \tag{3.6}$$

Subsequently, using Equation (3.1) a_{45} can be written in terms of θ,

$$\begin{gathered}{a_{45}}^2=\left[a_{01}+\left(2a_{12}-a_{23}\right)c\theta\right]^2+\left(a_{23}-2a_{12}\right)^2s^2\theta \\ \Rightarrow a_{45}=\sqrt{{a_{01}}^2+\left(2a_{12}-a_{23}\right)^2+2a_{01}\left(2a_{12}-a_{23}\right)c\theta}\end{gathered} \tag{3.7}$$

Finally, Equation (4.4) is used to define t_5 as a function of θ only,

$$t_5=\sqrt{{a_{45}}^2+{a_{01}}^2-2a_{45}a_{01}c\left\{\alpha-a\cos\left[\frac{{a_{01}}^2+{a_{45}}^2-\left(a_{23}-a_{12}-a_{34}\right)^2}{2a_{45}a_{01}}\right]\right\}} \tag{3.8}$$

By using Excel® solver tool, the optimization problem that is maximizing a_{23} by changing θ subjected to the constraints shown below is performed.

$$\text{Constraints: }\begin{cases}\text{Equations (4.1), (4.2), (4.3) and (4.4) must be satisfied}\\ t_5=10\,\text{mm}\\ \theta>30^\circ\end{cases}$$

For the initial value of $\theta = 31°$, the optimal a_{01}, a_{23} and a_{45} values are obtained as

$\theta = 37.7156$ deg
$a_{01} = 37.24$ mm
$a_{23} = 66.92$ mm
$a_{45} = 37.24$ deg

3.6. The Constructional Design of HiDAM

In this section, the designs of the part geometries that maximize the packing ratio are given, considering the design requirements and other constructional design deficiencies in the literature. In accordance with the design requirements received from STM company, the mechanism must be folded in a cylinder with a diameter of 90 mm and a height of 55 mm, and there are criteria such that its weight excluding the total useful mass is less than 200 g. As stated in the previous section, some constructional details in 2D should be included while creating the mathematical model of the structure due to the geometric boundary condition. However, since only the leg height, that is, the open height of the structure, can be improved in 2D, the constructional design in 3 dimensions (3D) is also of great importance in order to reduce the closed state height of the structure as the close height is equal to the sum of the heights of the overlapping hubs. The solid model of HiDAM parts and its assembly modelling are made using the SolidWorks® program, and a single deployable unit that realizes required Borel-Bricard motion, which means the top platform has only a translational motion with respect to the fixed bottom platform, is shown in Figure 3.7.

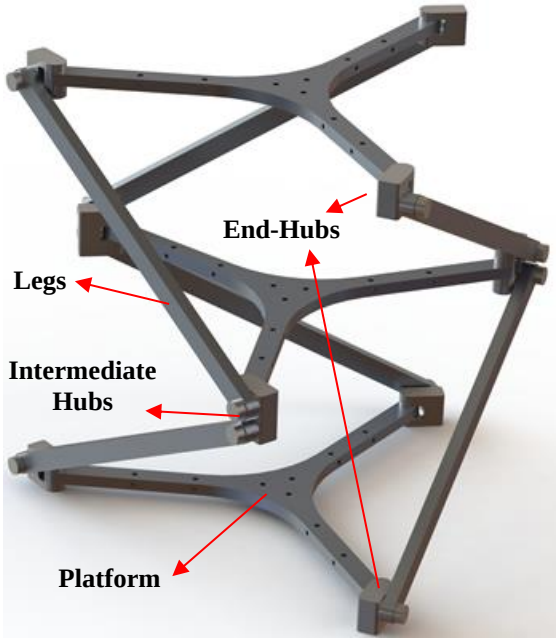

Figure 3.7. The single deployable unit of HiDAM

The Wren platform realizes two DoF when the legs become parallel to each other (Kiper and Söylemez 2011). It is a singular position, and the Wren platform no longer executes the Borel-Bricard motion after reaching to singularity Figure 3.8 (a), and the moving platform can be movable on a spherical paths while remaining parallel to the fixed platform Figure 3.8 (b).

a) b)

Figure 3.8. HiDAM in a) fully deployed position (singular configuration), b) two-DoF mode

HiDAM includes three types of parts in total. These are platforms, legs and hubs as seen in Figure 3.9. However, since the hubs connected to the first and last platforms need a single leg connection to reduce the closed state height of HiDAM, these hubs have a single leg joint and therefore their height has been reduced. Therefore, the hubs having one leg connection are called end hubs. In Figure 3.9, the exploded view of the 3 main elements forming HiDAM on the assembly is given. Washers are also used as a separator where legs are connected to hubs to reduce friction, and headed and flat screws are used to connect the parts where relative motion occurs.

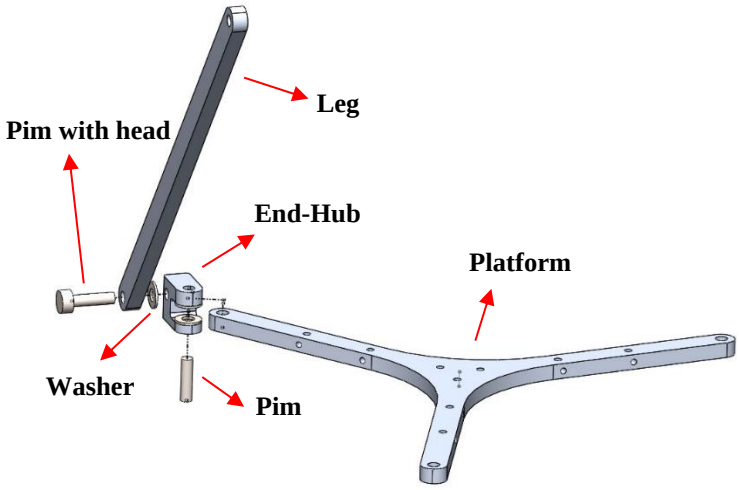

Figure 3.9. The elements used in HiDAM design in the exploded CAD view

3.6.1. Material Selection for HiDAM Parts

While choosing the materials for the parts of HiDAM, the list of suitable materials for space applications proposed STM company according to the ECSS-Q-ST-70-36C catalog from the European Space Agency standards was taken as a basis. For example, 316L type with high corrosion resistance is recommended for steel materials. It is necessary to pay attention to the cold-welding factor that may occur due to the use of similar parts together in the vacuum environment in space. It has been suggested by STM that nickel steel may be preferred for expansions caused by temperature change. For aluminum materials, 6061-T6 and 7075-T6 aluminum alloys with high corrosion resistance are recommended. Another issue to be considered in aerospace applications is the release of gases in the vacuum environment named outgassing. Therefore, for example, the use of brass material in space applications is not appropriate.

According STM, it was stated that alodine or anodized coating is applied to aluminum parts for corrosion protection. The coating type can be selected in accordance with requirements such as electrical conductivity and friction wear. Passivation process can be applied to steel materials, and then molybdenum disulfide (MoS2) can be used as a dry lubricant, especially for steel surfaces that will work with each other.

3.6.2. Platform Design

The outer circle dimension of the platform, for which three-branched star geometry was decided, was calculated according to the mathematical model. The platform has revolute joints positioned at the end of each branch to join hubs. In addition, there are holes in each arm to connect the cables, which are both elements of the actuation system and increase the stiffness of the structure. In the middle of the platform, there is a hole for anchor cables. Also, there are mechanical limit offsets to mechanically limit the deployment in fully deployed form to prevent the configuration change of HiDAM as shown in Figure 3.10. As the platform material, 7075-T6 aluminum alloy containing zinc as the primary alloying element was chosen, considering the weight criterion and its corrosion resistance properties.

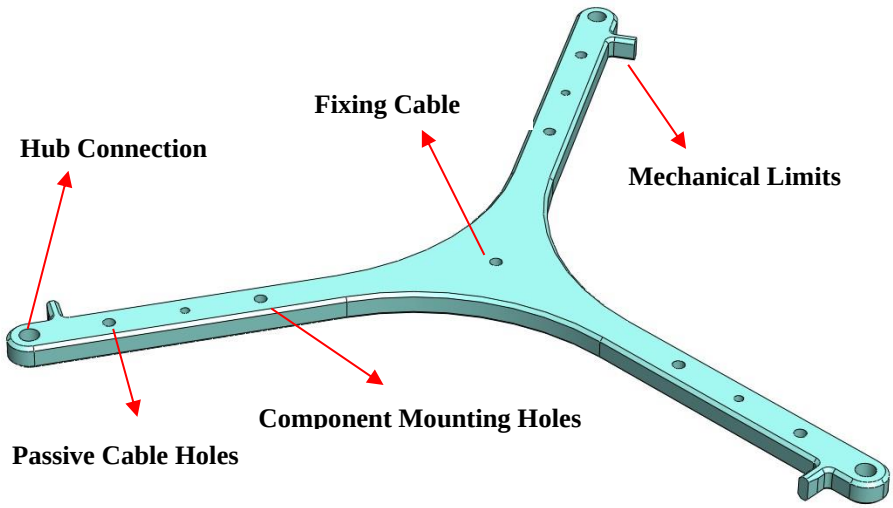

Figure 3.10. CAD Model of the Platform

3.6.3. Hub Designs

As in the platform design, a 3D constructional design was carried out for the hub designs, taking into account the 2D design determined in the mechanism design. As the end hubs need only one leg connection, their design is altered compared to hubs to reduce their heights as much as possible since the total height of the overlapping hubs is the only

factor that determines the stowed height of HiDAM Figure 3.11 (a). There are two revolute joints parallel to each other for intermediate hubs as seen in Figure 3.11 (b), where the legs will move relative to each other. There is another revolute joint perpendicular to these joints in each hub and it provides relative movement with the platform. Leg and platform connections are designed to keep the hubs' height to a minimum. By designing a u-shaped mouth to connect the platform from above and below, the connection with the platform is ensured in a way that requires minimum height. In the connection of the legs, a minimum gap is left between the holes to prevent the end points of the legs from colliding with each other. As the material, steel 316L, one of the materials recommended by STM, was chosen, to have higher strength during chip removal and thread cutting process.

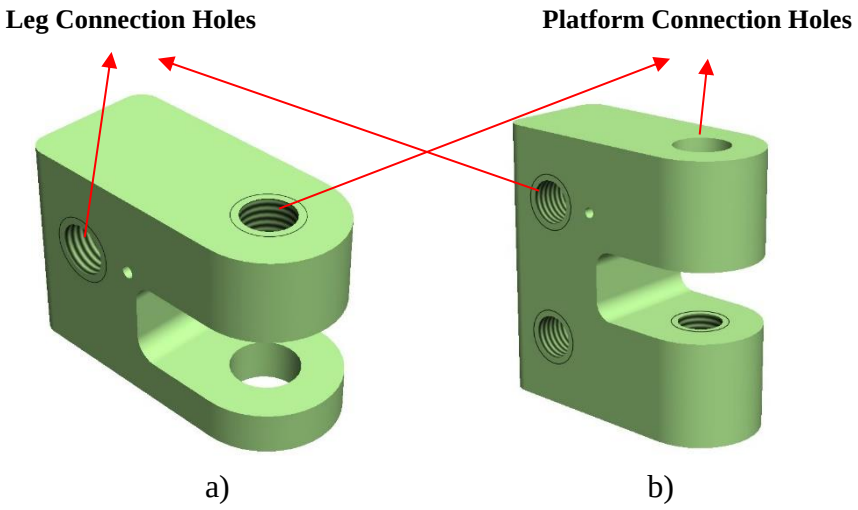

Figure 3.11. CAD model of the hubs a) end hubs, b) intermediate hubs

3.6.4. Leg Design

The legs act as a part connecting the two platforms, thus enabling the platforms to move relative to each other. The legs connected to the hubs of two consecutive platforms have revolute joints where they are attached to the hubs as shown in Figure 3.12. The main aim of the developed mathematical model in 2D is to maximize the effective leg length which is the distance between two revolute joints of the leg. Hence,

it is calculated to be the highest value by optimization, that is 66.92 mm. Like other parts whose dimensions are calculated according to the mathematical model, the precision of the distance between two revolute joints is crucial to prevent contraction in the movement of the mechanism. Moreover, a rectangular cross-section structure has been designed as it will provide an advantage in the drilling operation of the leg. Aluminum 6061-T6 was chosen as the material, again due to its high hardness and strength properties. The sharp ends of the legs have also been chamfered to both reduce mass and prevent collisions.

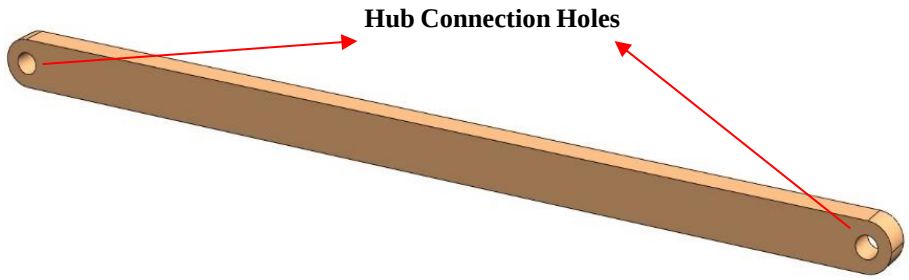

Figure 3.12. CAD design of the leg

3.6.5. Fasteners

While the legs are connected to the hubs via M1.6x0.35 headed screws to hold the legs and hubs together, the connection of the platforms to the hubs through a u-shaped void is carried out by using M1.6x0.35 screws, which are can be seen in Figure 3.13 (a) and (b), respectively. However, the thread length of these screws is specified according to the allowable thread-cutting lengths on hubs, thus they must be custom-made parts. For the material of these screws, steel 316L is decided considering its high strength characteristics.

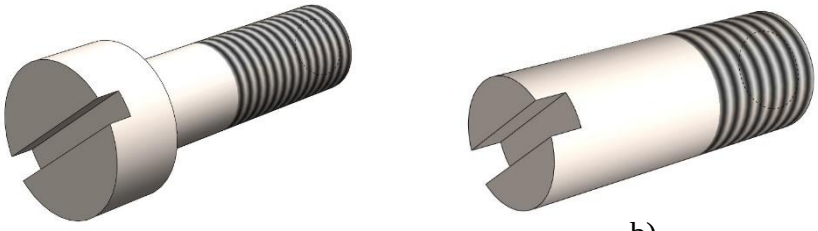

a b)

Figure 3.13. The custom-made screws a) headed screws, b) flat screws

The heads of the screws are grooved to ease the assembly process by using appropriate tools. Moreover, the connections are further secured via bonding with epoxy. These connections could be carried out by using pins with tight fit, however, considering the thermal expansion in space conditions, screws are chosen to have a redundant safety. Furthermore, the connection between legs and hubs is separated via DIN433 M1.6 washers to minimize the additional frictions that will occur due to the rubbing of the hub and leg surfaces against each other.

3.7. Actuation System Design of HiDAM

In this section, the actuation system design and its components are presented. This work is carried out by Murat Demirel, who is also a researcher in the TÜBİTAK 1005 project. The actuation system of a DTM can be designed as retractable or only deployable. While the retractable DTMs can switch between its open and close configurations, the deployable DTMs can only be deployed to its open positions once. Within the scope of the actuation system design studies, first of all, the existing ones used in DTMs in the literature and the springs used for the revolute joint actuation are examined.

When the existing applications are examined in detail, it is seen that only compressed springs of the deployable type (i.e., torsion springs, spiral springs, or compression springs) can transmit motion. In structures with this type of actuation, most torsion springs are used. Vorlicek et al. (1982), Wie et al. (1986), Nataraju et al. (1987) and Celli et al. (1990) are examples of deployable masts using a such actuation system by torsion springs. In Figure 3.14, the spring and cable details of the actuation system designed by Vorlicek et al. (1982) are shown. Torsion springs, here, provide the drive of

the revolute joints. The cable loops connected over pulleys placed on these joints help the simultaneous movement of the joints and limit the movement once deployed to an open position.

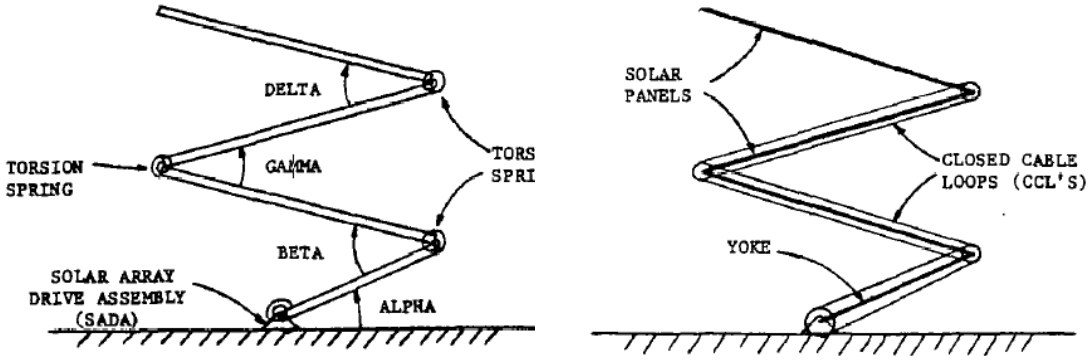

Figure 3.14. A space application with torsion spring and closed-circuit cable system (modified from Vorlicek et al. 1982)

There are also deployable mast examples in which spiral springs are used as an actuation system. For instance, Watt and Pellegrino (2002) presented a revolute joint driving system using spiral springs as shown in Figure 3.15. Shan et al. (2013) also used this type of spring in their DTM proposal, which is presented in Figure 2.7 (c). The design of revolute joint actuation system with spiral springs is extensively studied by Pellegrino et al. (2000).

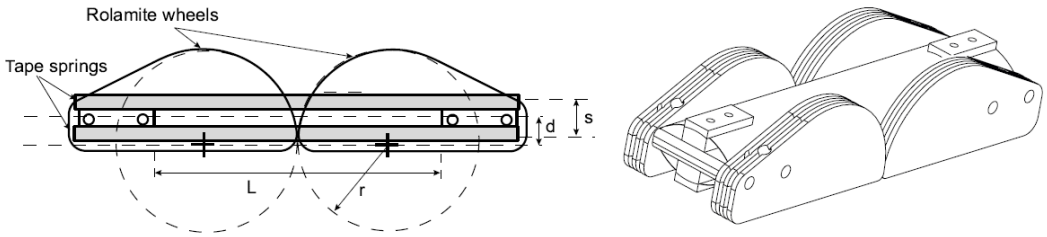

Figure 3.15. An example of revolute joint actuation system with spiral springs (Watt and Pellegrino 2002)

For retractable structures, the movement is provided with the help of cable-driven actuators. In systems with active cable, where the cable length changes, actuators can

only transmit tensile forces. Therefore, in such systems, one cable-pulley system is used for the movement between the closed and open position and the other for the reverse movement. An example of such an actuation system is shown in Figure 3.16 (Kumar and Pellegrino 1996).

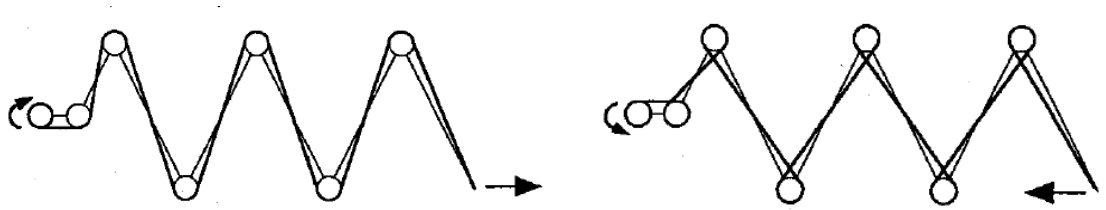

a) b)

Figure 3.16. The cable-driven actuation system proposed by Kumar and Pellegrino (1996), a) deployment cable, b) retraction cable

These cables, which can be called deployment and retraction cables, transfer the movement between the parts of the deployable structure to be driven with the help of free-turning pulleys fixed on the joints and terminate on a pulley connected to the motor. In this case, the movement of the mechanism can be controlled by at least two motors. Again, since it is recommended to use the cable systems redundantly for both load distribution and preventing any problems, the number of motors can increase to four. Figure 3.16 (a) shows the deployment cable and Figure 3.16 (b) shows the retraction cable. In both cases, the desired movement is obtained by shortening the cable lengths.

3.7.1. The Springs Used to Drive Revolute Joints

Torsion springs are the types of springs that are generally used for the driving of revolute joints. They resist the forces that create rotation and torsion. These springs store potential energy while compressing it. This energy is transferred, and movement is provided by the rotation of one of the spring arms with respect to fixed arm in the opening direction. Torsion springs can have spring ends in various forms (Figure 3.17) as short hook ends, hinge ends, straight offset and straight torsion. It is essential that these springs need to be designed considering that they are being loaded while closing.

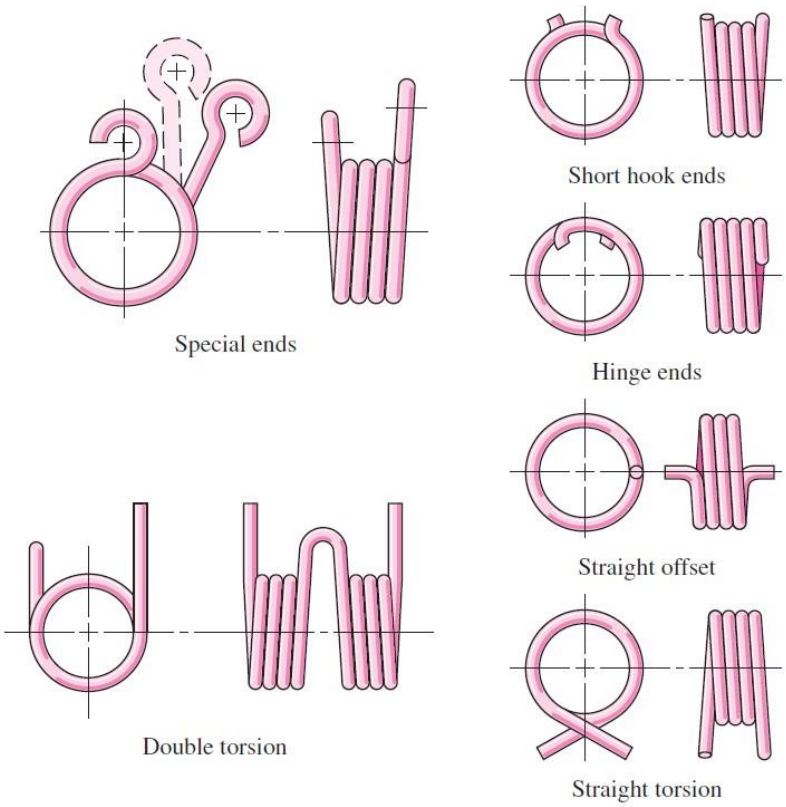

Figure 3.17. Torsion springs and its end types (Budynas et al. 2020)

Given the fact that spiral springs require higher displacement and compression springs have drawbacks in terms of assembly calibration, torsion springs are the most common and appropriate solution to actuate the revolute joints. Considering the leg movement with respect to hubs, it is decided that the fixed arm of the torsion spring is located on hubs and the free arm on the legs. Since there are three leg-hub connections for each platform, simultaneous deployment can be achieved by designing a torsion spring actuation system that will drive the revolute joint on each of the three legs. This set of actuation system on each platform can be repeated for other platforms to ensure that the driving system is redundant and will provide flexibility in obtaining the required torque. Taking into account the HiDAM's dimensions, it is suitable to release the cable that keeps the structure in its close form by cutting it. In these type of drive systems, the movement of the mechanism is achieved by cutting the fixing cable with the help of a heated resistor like a thermal knife. Considering the structure of HiDAM, this cable must be fixed on the first and last platforms, otherwise movement may occur in the closed position.

3.7.2. Torsion Spring Design for Actuation

Due to the size of the torsional spring that is suitable for HiDAM is out of standards, it is designed to be custom-made. Thus, the design parameters shown in Figure 3.18 are used. Based on the design parameters, the wire diameter, moment arm, fixed arm length, body length of the spring and angle of twist are selected so as to meet the desired torque requirements. Since wires are shaped by molds, non-standard moment-arm geometry can be designed as desired.

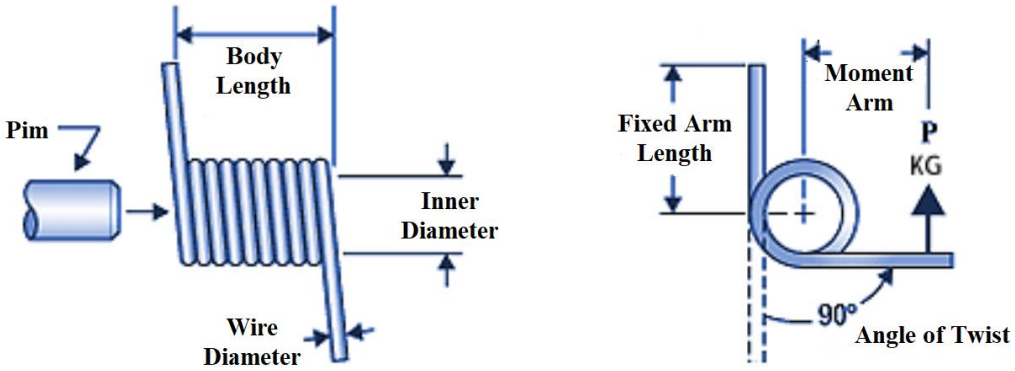

Figure 3.18. Design parameters for a torsional spring (modified from Tekno-Tel Yay 2022)

The inner diameter of the mandrel and the angle of twist can be determined from the constructional details. The revolute joint where M1.6 headed screws are used for connections is selected for actuation. The length of the headed screws where torsion springs are attached kept longer for housing. Thus, the torsion angle can be determined according to the amount of rotation between the leg and the hub, to which the pin is attached.

To actuate HiDAM from its close position to fully deployed state requires 90° rotation of legs with respect to hubs. As the free arm of the torsion spring is located on the leg, that arm needs to have at least 90° angle of twist. However, in the fully deployed state of HiDAM, self-motion occurs at the legs, which causes a configuration change, and the structure can move like a parallelogram as mentioned in Section 3.6 and shown in Figure 3.8 (b). Nevertheless, the singular configuration is advantageous in terms of

stiffness, thus, the deployment should be as close to the fully deployed state as possible. By designing the torsional spring having more than 90 degrees angles of twist and limiting the structure by means of mechanical stops and cables creates an increase in the stiffness since the spring would be restricted in motion at an angle value less than the angle of twist and the remaining potential energy would give additional resistance to the structure.

Considering the size constraints of HiDAM, the spring parameters listed in Table 3.2 was taken as a reference spring (The Spring Store 2022). These parameters are given for the free state of the spring as standard. The angle of twist increases as the body length or the number of turns increase in springs with the same mandrel diameter and inner diameter. In other words, the amount of potential energy that the spring can store increases. Accordingly, the body length of the spring designed for a wire diameter of 0.3 mm and a torsion angle of 90° was determined as 1.91 mm and the number of turns as 5.25. As mentioned before, since HiDAM is suitable for use of redundant springs, it is not necessary to calculate required torque.

Table 3.2. Reference Torsion Spring Parameters (The Spring Store 2022)

Inner Diameter (mm)	**Mandrel Diameter (mm)**	**Fixed arm length (mm)**	**Wire Diameter (mm)**	**Body Length (mm)**	**Number of Turns**	**Twist Angle (°)**	**Torque (N·mm)**
2.057	1.524	9.652	0.305	1.524	3.25	72	4.180

Three alternative springs are studied in the open position of the leg according to the selected spring parameters and the design alternatives are shown in Figure 3.19. Among the design alternatives, the first design is chosen since it provides larger surface contact area on the leg which helps to enhance the force transmission. Also, the arm geometry in the first design does not cause any interference with the hub and platform during any state of the deployment.

The details of the arm geometry of the designed spring are represented in Figure 3.20. As the moment arm length of the free arm where the spring is attached to the leg increases, the amount of torque generated in the actuated joint increases, however bending

of the arm should be considered as well. Therefore, considering the possible overlaps of the parts, the moment arm length is chosen as 6.50 mm. The resulting assembly is illustrated in Figure 3.21.

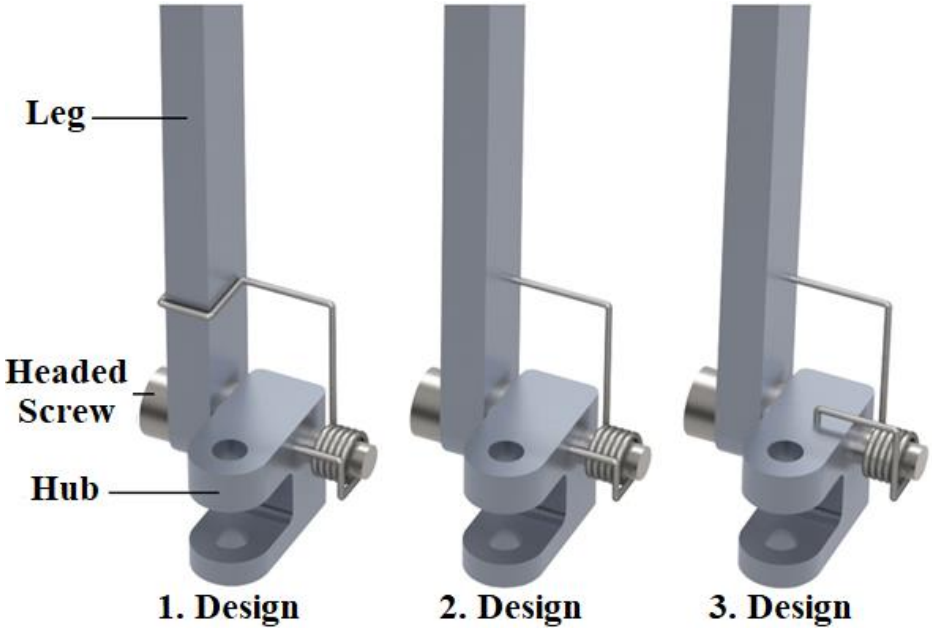

Figure 3.19. Design alternatives for torsion spring

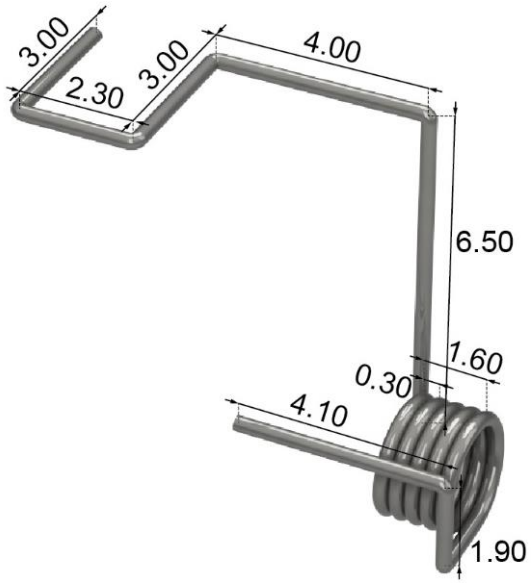

Figure 3.20. Dimensions of the custom-designed torsion spring

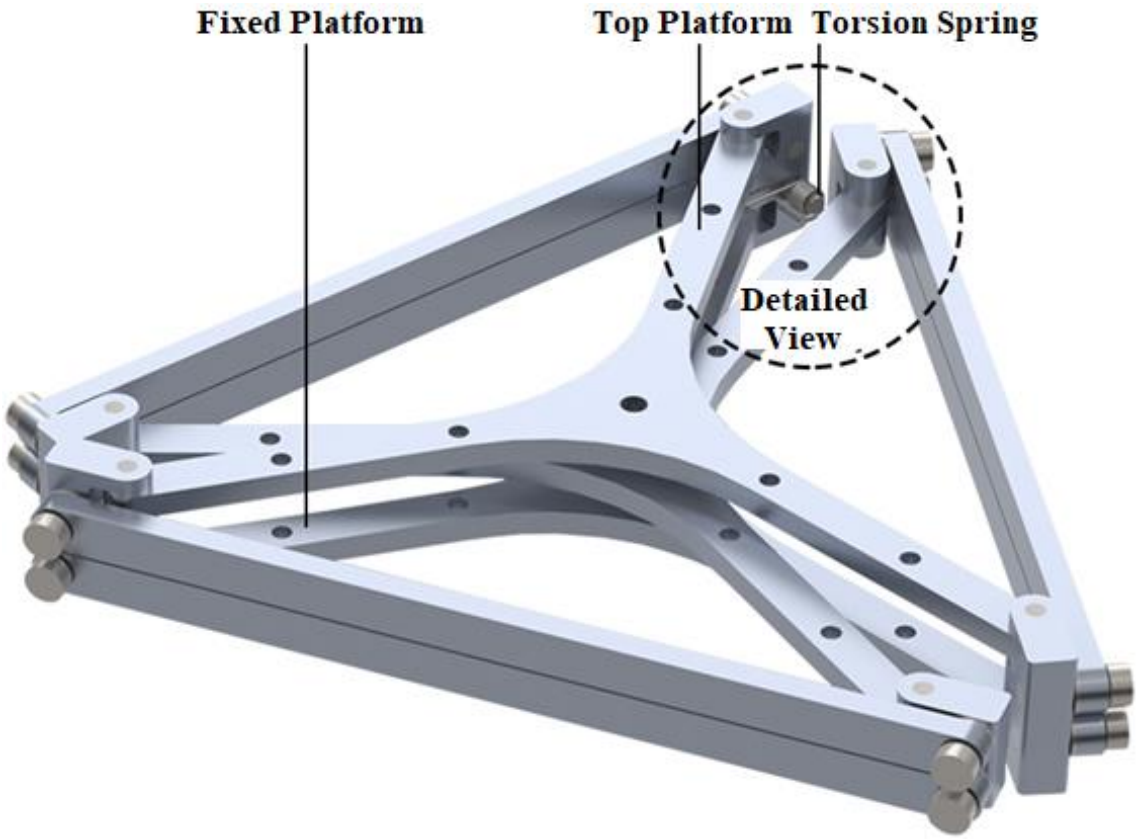

a)

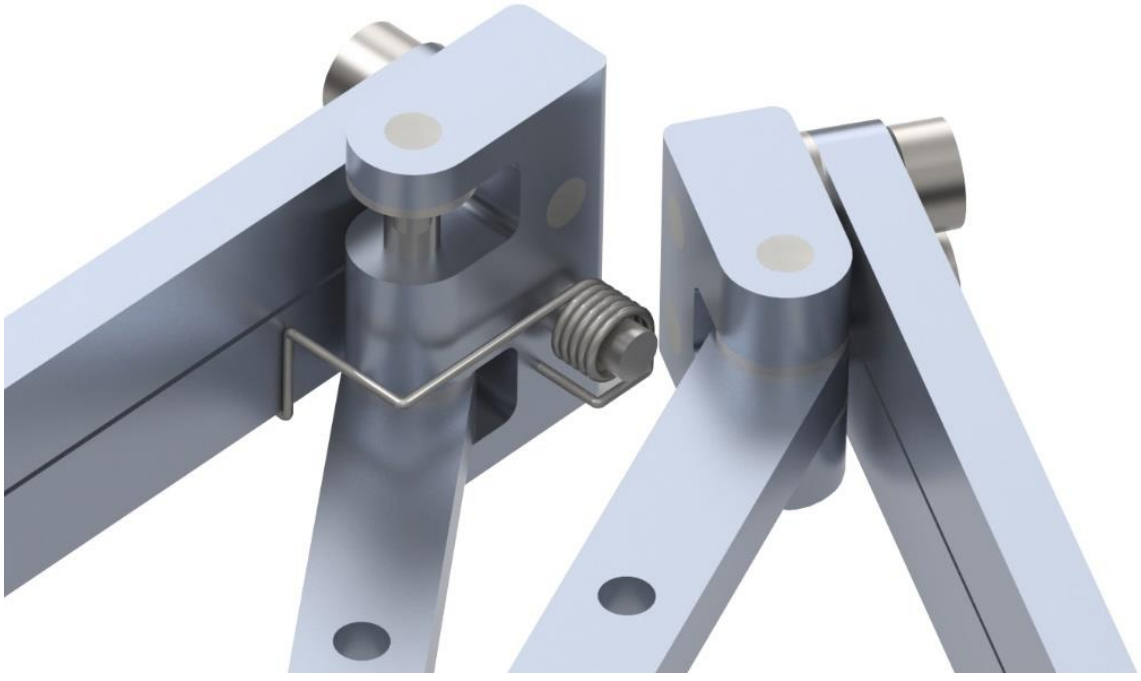

b)

Figure 3.21. The torsion spring assembly to a deployable unit of HiDAM in the a) stowed position, b) detailed view of the torsion spring assembly where the top platform is hidden

3.7.3. Design of Passive Cable Elements for HiDAM

As discussed before, active cables can be used to actuate the deployable masts to control and retract the structure when necessary. However, passive cables are also needed to limit the deployment and most importantly to enhance the stiffness of the mast. The length of the passive cables does not change compared to active ones, and they are loose when the structure is stowed. The key point in using multiple passive cables is to ensure that all cables must be tight when the mast is fully deployed (Figure 3.22). The usage of cables in deployable masts is discussed by Kwan et al. (1991).

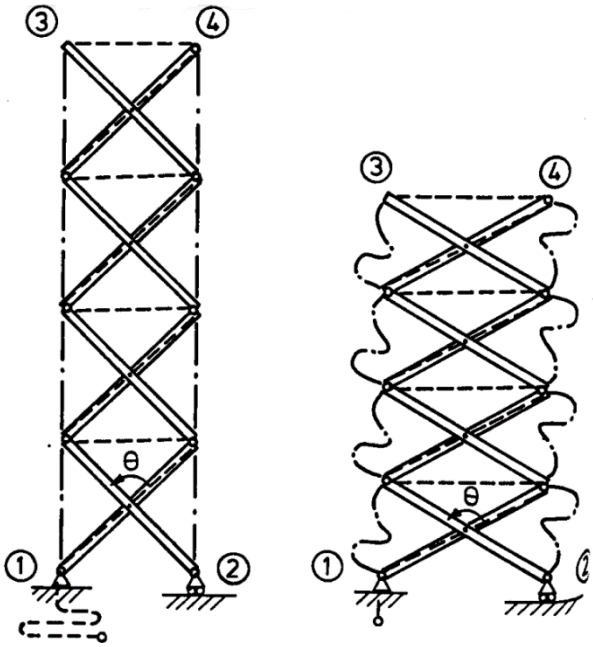

Figure 3.22. Schematic representation of active and passive cables (Kwan et al. 1991)

In HiDAM, it is decided to use two passive cables, one is to enhance the stiffness and limit the structure, the other is to hold HiDAM in the stowage state. The use of the first passive cable allows each platform to be connected to another platform. Cable holes drilled on the platforms are concentric throughout the movement on odd or even numbered platforms. That is, the first passive cables pass through either odd-numbered platform only or even-numbered platform. The positions of the cable holes are adjusted so that the cables of the odd and even number of platforms do not interfere with each

other. Figure 3.23 shows the example for the connection of the first passive cable between the first and third platforms, that is, between the fixed and end platforms, for the open state of a module. It is crucial to distribute the load equally for each cable. In this way, all platforms can be connected to each other with two sets of three cables. The length of these cables also limits the deployment and determines the open position of the HiDAM to have a redundant system for the mechanical limit. It is important that the cables are set at equal tension in the open configuration. This can be achieved by installing cables in equal lengths. Therefore, after bringing HiDAM to the desired open position, these cables should be mounted in equal lengths. For this, precise marking must be made from the desired termination points on the selected cable and the assembly must be carried out precisely.

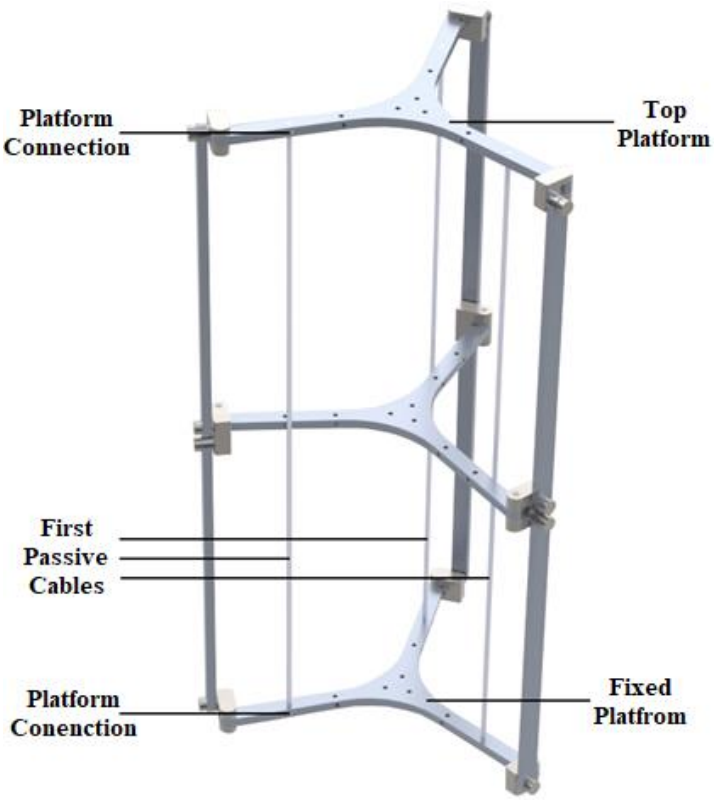

Figure 3.23. Passive cables to increase stiffness and limit HiDAM

For the second passive cable, it is aimed to keep the HiDAM in the closed position and to release the structure by cutting this cable. As shown in Figure 3.24, the cable is connected to the fixed and end platforms of the six-module HiDAM through centers of

the platforms. The center holes are concentric throughout the structure on all platforms and there is no odd or even platform separation as in the first cable use. The cable, which is fixed to the fixed platform by means of M1 setscrews, will be terminated on the end platform with a cable termination element as shown in the figure. During assembly, the cable connected to the end platform with the cable terminator will be fixed by stretching over the fixed platform in the closed position of HiDAM. Here, it is important to provide sufficient pre-tension to the mechanism in the closed position. For both passive cables, fluorocarbon cables are chosen because of their durability, wear resistance and low flexibility features (Berkley Fishing 2022).

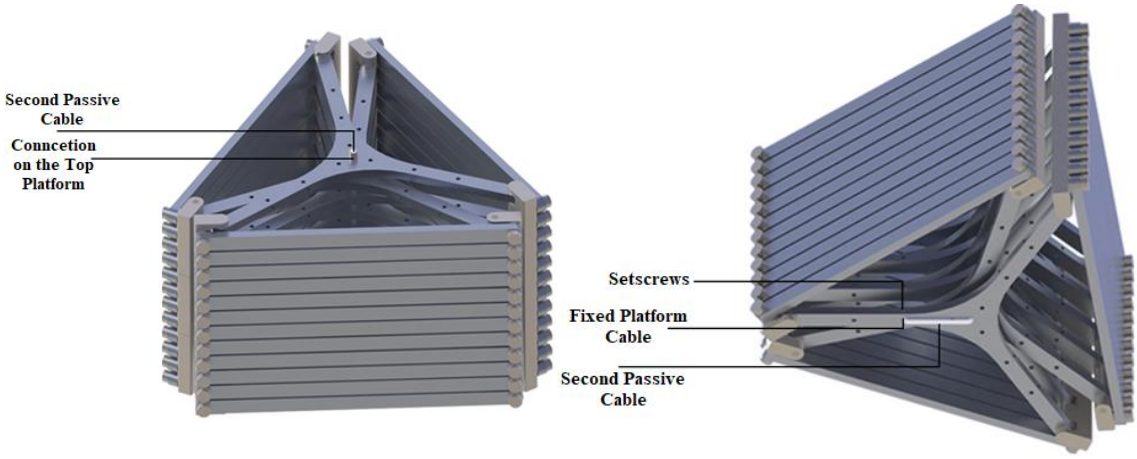

Figure 3.24. Second passive cable a) top platform connection, b) fixed platform connection

3.7.4. Control Unit of The Actuation System

The details of the control unit to be used in the prototype of the HiDAM are shown in Figure 3.25. An SMD resistor circuit is used as a thermal blade in the actuation system control. The power supply of this circuit will be sent with the relay circuit to which the National Instruments myRIO controller card is connected (myRIO, 2022). Due to the redundant actuator requirement of space applications, two resistors will be used for one cable. The resistor will not exceed the set current value if the current limiting circuit element is used in the resistor circuit as the temperature rises and the quantity of current

drawn rises, the value of the resistors falls. Thanks to the actuation signal sent from the myRIO controller, a relay will open the power supply to which the resistor circuit is connected, and the cable will be cut by the heat of the resistor generated.

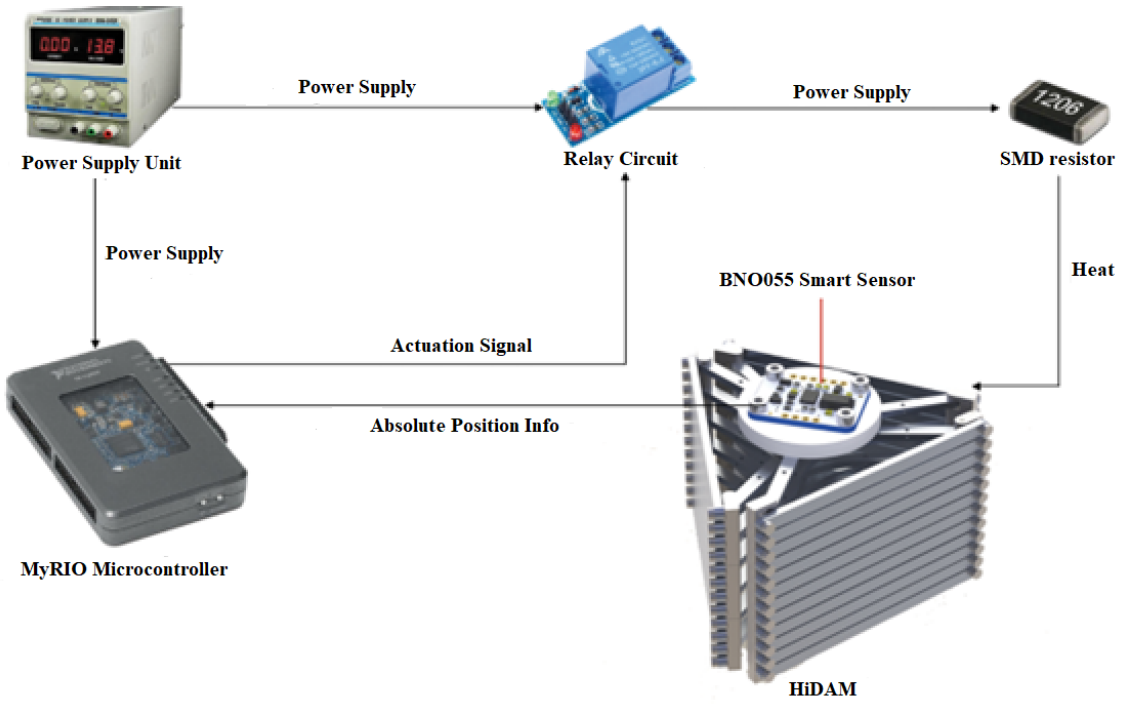

Figure 3.25. Control unit of the actuation system of HiDAM

CHAPTER 4

PROTOTYPE OF HIDAM

In this Chapter, the manufacturing of the HiDAM parts and one deployable unit assembly is given. One of the main challenges in manufacturing was to find an appropriate manufacturer as the part sizes are out of standards for most of the companies and on the budget of the project. This Chapter comprises two design iterations and the assembly of the single deployable unit is performed for the second design iteration.

4.1. Manufacturing of parts

An initial prototype (Prototype A) is manufactured based on the initial design. After design iterations and preliminary tests, a second prototype (Prototype B) has been manufactured. The two prototypes are presented below.

4.2. Prototype A

After the constructional design of HiDAM, the parts are manufactured. This process required a tremendous amount of time to find the appropriate manufacturer, which is skilled enough to machine small-size parts, for example, drilling 0.5 mm diameter holes, thread cutting for M1.6 screws etc. First, the platforms are manufactured by the wire erosion method since it provides high precision and improved surface finishes, and it is an appropriate technique for contour cutting. The manufactured platforms can be seen in Figure 4.1. As mentioned in the constructional design section, there are two types of platforms, without mechanical limits and with mechanical limits as seen in Figure 4.1 (a) and (b), respectively. The most important dimension for platform is the distance from the center to the revolute joint holes on each arm as it is where the hub is connected to

the platforms. The precision is kept at +/- 0.02 mm for the distance from center to revolute joint centers at the arm ends and +/- 0.05 for the holes itself.

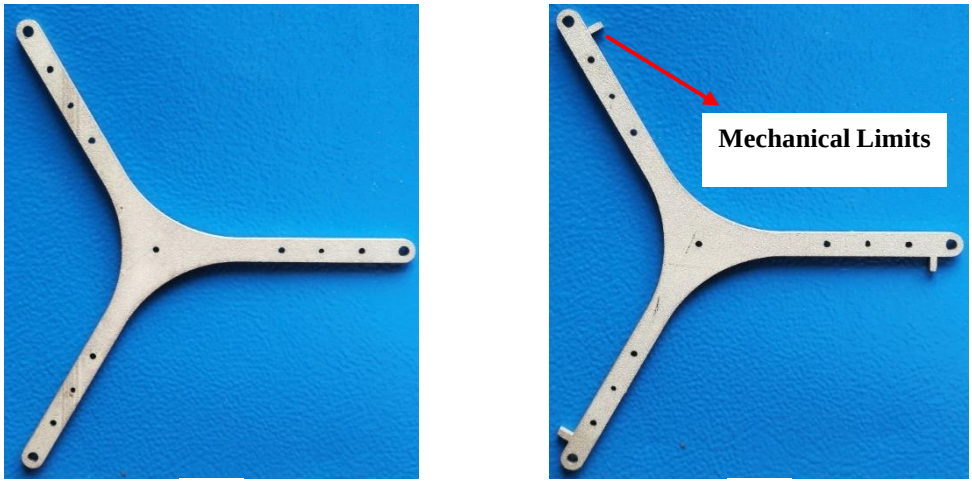

a) b)

Figure 4.1. Manufactured platforms with a) no mechanical limits, b) mechanical limits

As for the hubs, CNC vertical processing center is the most appropriate option since it requires machining on several surfaces. The manufactured hubs are shown in Figure 4.2. As in platforms, there are two types of hubs, intermediate and end hubs as seen in Figure 4.2 (a) and (b), respectively.

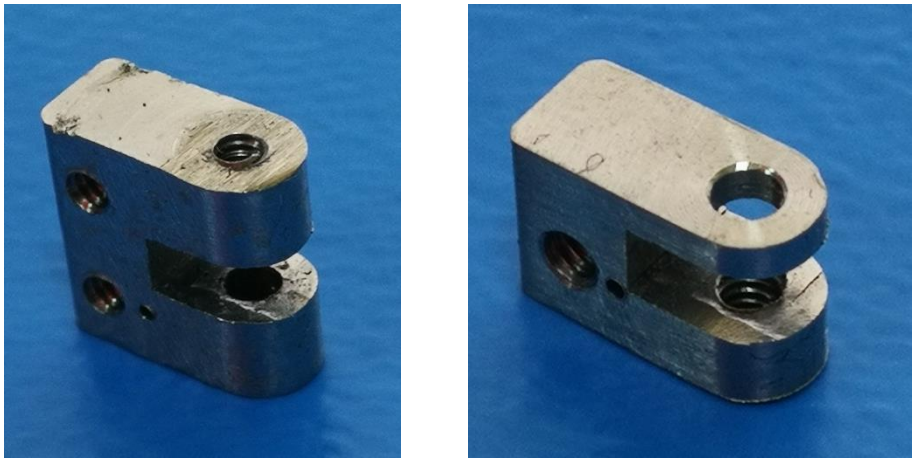

a) b)

Figure 4.2. Manufactured a) intermediate hubs, b) end hubs

The legs are also manufactured by wire erosion method like platforms as represented in Figure 4.3. The crucial parameter for the legs is the revolute joint center distance as they are used to connect consecutive platforms and play and important role in the movement of structure.

Figure 4.3. Manufactured leg

The fasteners such as screws are manufactured by CNC lathe as shown in Figure 4.4. There are two types of screws, flat and headed as shown in Figure 4.4 (a) and (b), respectively. The DIN433 M1.6 washers are purchased.

a) b)

Figure 4.4. Manufactured pins a) flat screws, b) headed screws

4.3. Prototype B

After Prototype A, some parts of the HiDAM are altered based on the deployment and functional performance of the single deployable unit. First, to enhance the stability of the structure at the stowage configuration, the star-shaped platforms are changed to a triangular form without changing the size of the design parameters. As in Prototype A, mechanical limits are preserved. Additionally, on each side of the triangle, some specific sections are leveled to fill the gaps between platforms in the stowage configuration. It is seen that five platform types are needed for the 6-module assembly considering mechanical limits and levelled sections as shown in Figure 4.5. Unlike the other four types, the 1st platform is not hollow since the microcontroller that is used to cut the releasing cable should be mounted on it.

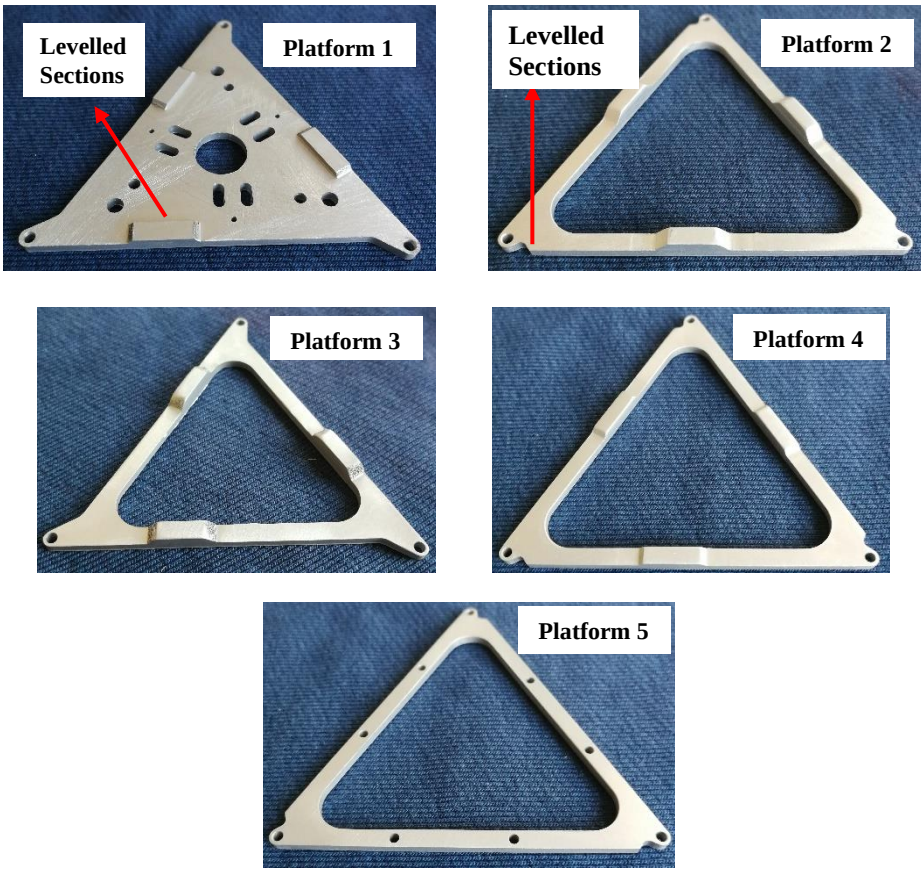

Figure 4.5. Manufactured five platform types

As for the hubs, the passive cable holes are placed at the back of the hubs, which are located at the most outer section of the mechanism in order to maximize the stiffness of the structure when it is fully deployed, as represented in Figure 4.6.

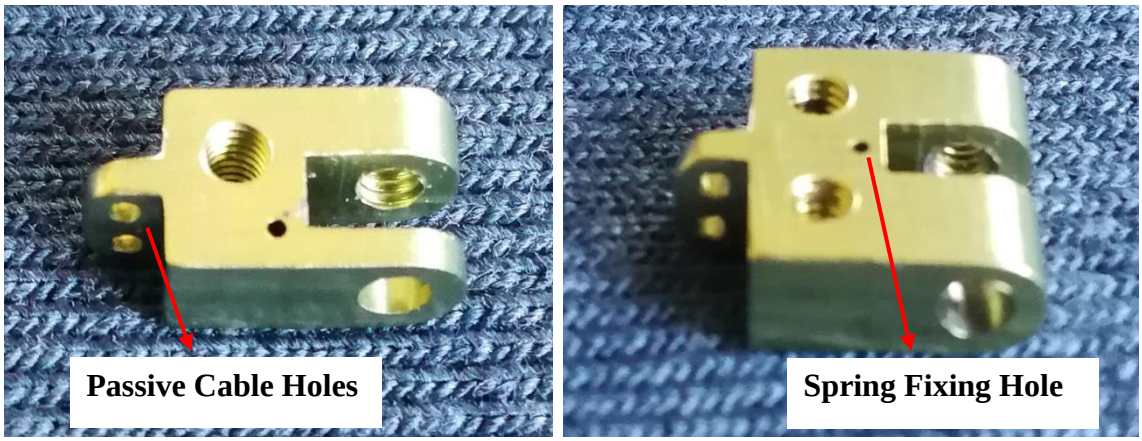

a) b)

Figure 4.6. Manufactured hubs with passive cable holes a) intermediate and b) end hubs

The legs are redesigned to have a circular cross-section to increase the bending resistance while keeping the flat surface at the ends as seen in Figure 4.7. Unlike the previous legs, these are manufactured using CNC machines.

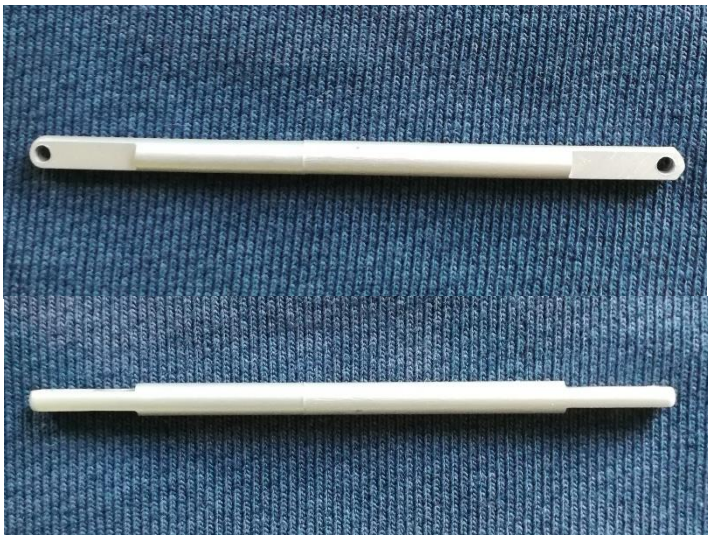

Figure 4.7. Manufacturing of the altered leg

Figure 4.8. Manufactured pins for the second design

As for the screws, which are of four types, they are grooved at one end to ease the assembly with the screwdrivers, and they are changed to M1.8x0.35 type. The four types of the screws are shown in Figure 4.8.

Finally, all the precision requirements are kept same with the prototype A and material of the hubs and screws are changed from steel 316L to Ti 6Al 4V to lower the mass and enhance the strength.

4.4. Assembly of Single Deployable Unit of HiDAM

After the manufacturing of parts and purchasing of washers, the assembly is done at IzTech Rasim Alizade Mechatronics Laboratory for the single deployable unit for both design iterations. Figure 4.9 shows the front and top view of Prototype A assembly in its fully folded configuration.

a) b)

Figure 4.9. Stowed configuration of 6-module assembly of HiDAM a) Front view, b) Top view

In Figure 4.9, it can be seen that the end hubs overlap, and the intermediate hub is located next to them. Next, the semi-deployed state is represented in Figure 4.10 (a) along with the spring actuation system detail in Figure 4.10 (b). The deployed assembly is shown in Figure 4.11.

a) b)

Figure 4.10. Single deployable unit of HiDAM a) semi-deployed configuration, b) spring actuation system detail

a) b)

Figure 4.11. Single deployable unit of HiDAM in fully deployed configuration a) vertically deployed, b) horizontally deployed

For the second design, the assembly is done with the altered parts and its folded, semi-deployed and deployed configurations are shown in Figure 4.12. Also, a 6-unit prototype is manufactured (Figure 4.13).

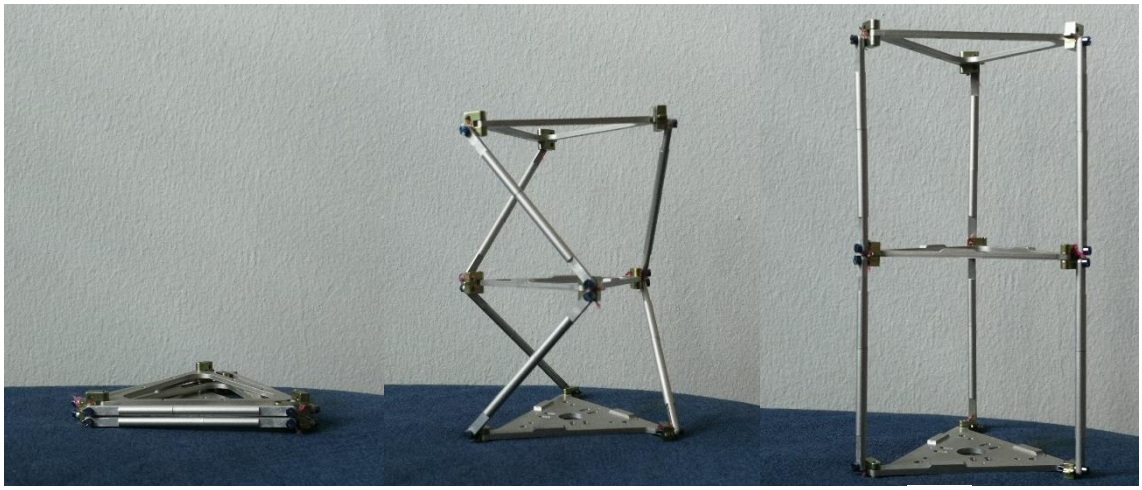

a) b) c)

Figure 4.12. Single deployable unit of HiDAM based on Prototype B in a) folded, b) semi-deployed and c) deployed configurations

a) b)

Figure 4.13. 6-unit prototype of HiDAM in a) folded, and b) deployed configurations

CHAPTER 5

RESULTS AND CONCLUSIONS

The purpose of this study is to design a new deployable truss mast that has superior packing ratio compared to the examples in the literature. To achieve this, recent DTM examples are investigated, and a new design methodology is proposed. According to the proposed and prototyped DTM called HiDAM, the following achievements are obtained.

First, it is crucial to define how any two deployable masts are compared. In the literature, there are several unsatisfactory packing ratio comparisons. To be able to compare two deployable masts and to present a meaningful data, the allowable volume restriction should be equal and the deployable masts that are going to be compared should be of same type.

To calculate the packing ratio of HiDAM, the deployed and stowed height are calculated according to the following formulae:

$$\text{deployed height} = d = 2na_{23} + 2z + (2n-1)y = 853.1\,\text{mm} \tag{5.1}$$

$$\text{stowed height} = s = 2z + 2nx + (n-1)y = 50\,\text{mm} \tag{5.2}$$

where n is the number of deployable units, which is taken as 6 for HiDAM. The hubs parameters x, y and z are shown in Figure 5.1.

Thus, the packing ratio is the ratio of deployed height to stowed height, which is calculated as:

$$\text{packing ratio} = f = \frac{d}{s} = 17.06 \tag{5.3}$$

The packing ratio of the DTM proposed by Wang et al. (2022) has also 90 mm circumscribing diameter. Therefore, these two DTMs can be compared in a fair way. As they reported the packing ratio of their proposal as 15.17, it is proved that the packing ratio of HiDAM is about 12% better than the most recent DTM example published by Wang et al. (2022). The stowed and deployed view of 6-module assembly of HiDAM showing their heights can be seen in Figure 5.2 (a) and (b), respectively.

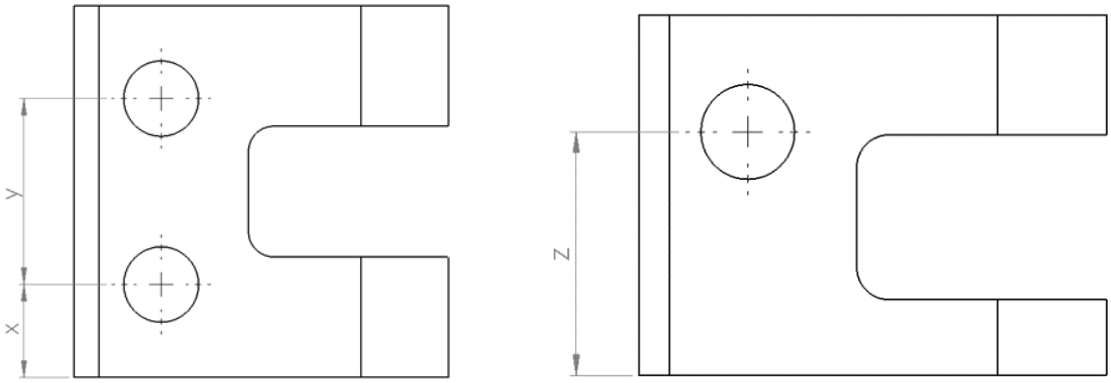

a) b)

Figure 5.1. The hub parameters for a) intermediate hub, b) end hub

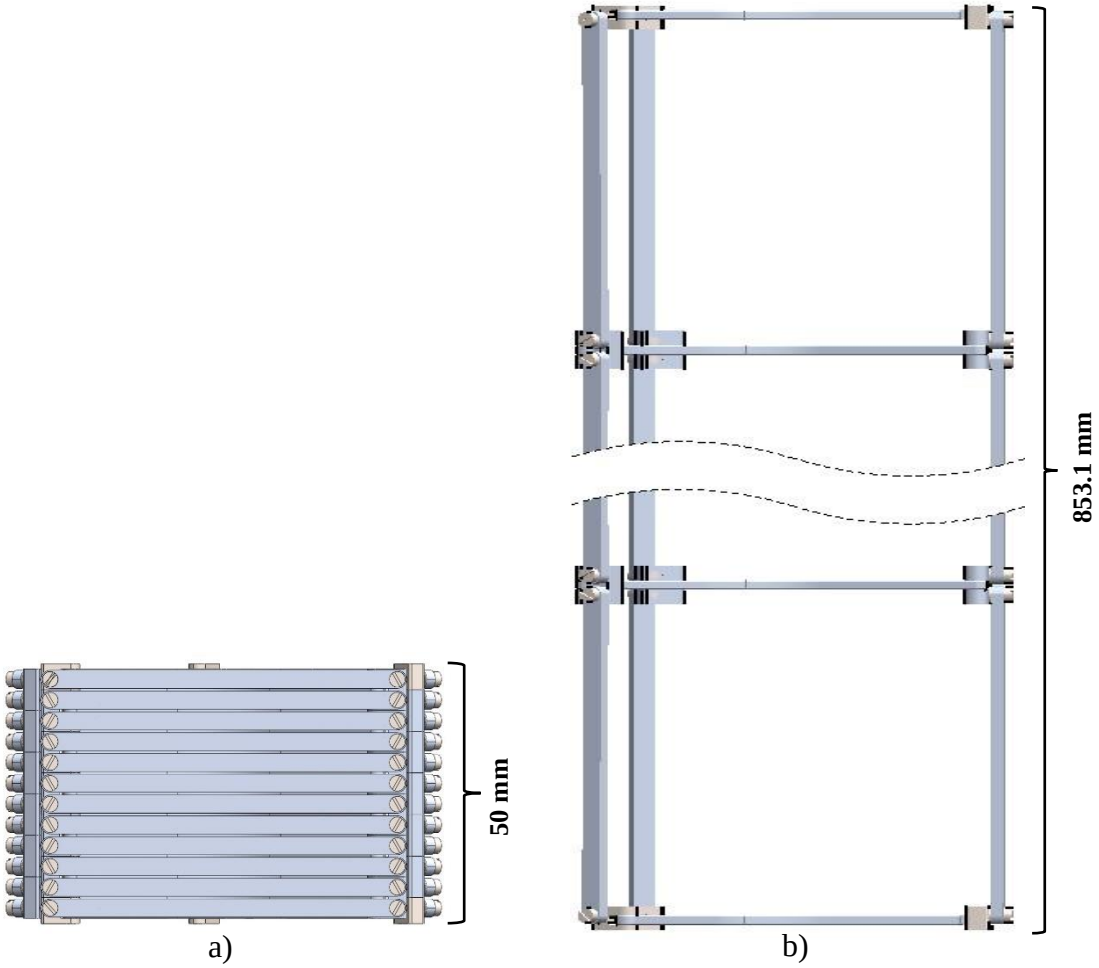

a) b)

Figure 5.2. 6-module assembly of HiDAM a) stowed state, b) deployed state

However, since the packing ratio is proportional to the circumscribing circle diameter and increasing it directly allows to use longer legs without changing other parts dimensions, which substantially increases the packing ratio. Hence, HiDAM is scalable to the extent that the strength of the leg permits.

As a result, HiDAM provides better packaging ratio compared to the similar structures used in aerospace applications. As represented in this thesis, the mathematical model allows to maximize the packing ratio by optimizing the part lengths according to structural analysis. As for future works, with further constructional design improvements the packing ratio can be increased.

REFERENCES

Belvin, W. Keith, Marco Straubel, W. Keats Wilkie, Martin E. Zander, Juan M. Fernandez, and Martin F. Hillebrandt. 2016. “Advanced Deployable Structural Systems for Small Satellites”. In NATO CSO STO Specialist Meeting AVT-257 /RSM-041 on Best Practices for Risk Reduction for Overall Space Systems, 26–29. Zaragoza: Applied Vehicle Technology Panel. https://ntrs.nasa.gov/api/citations/20170003919/downloads/20170003919.pdf.

Benton, Max D., and William M. Robbins Jr. 1986. “Extendible Structures.” U.S. Patent 4,599,832 issued July 15, 1986. https://patents.google.com/patent/US4599832.

Berkley Fishing. “Why Use Fluorocarbon?” Accessed July 6, 2022. https://www.berkley-fishing.com/pages/berkley-ae-why-use-fluorocarbon.

Borel, Émile M. 1905. “Mémoire sur les Déplacements à Trajectoires Sphériques”. Imprimerie Nationale.

Bricard, R. 1896. “Géométrie cinématique—sur un déplacement remarquable.” Comptes-Rendus de l’Académie des Sciences, Paris 123, no. 22

Budynas, Richard G, J Keith Nisbett, and Joseph Edward Shigley. 2020. Shigley’s Mechanical Engineering Design. New York, NY: McGraw-Hill Education.

Cebeci, Yunus, Murat Demirel, and Gökhan Kiper. 2022. “A Critical Review of Deployable Truss Masts and Proposal of a New Mast: HiDAM.” In International Symposium on Unmanned Systems and the Defense Industry (ISUDEF’22), May 30-June 01, 2022. Madrid, Spain.

Cebeci, Yunus, Murat Demirel, and Gökhan Kiper. 2021. “Katlanabilir mafsallı kafes direklerin katlanma oranlarını etkileyen faktörlerin incelenmesi ve yeni bir tasarım yönteminin araştırılması.” In 20. Ulusal Makina Teorisi Sempozyumu (UMTS 2021), September 15-17, 2021. Diyarbakır, Turkey.

Celli, J., N. Lomas, H. Pollard, and N. Totah. 1990. “Intelsat VII solar array electrical and mechanical design.” In AIAA International Communication Satellite Systems Conference and Exhibit, 13th, 34-41, Los Angeles, CA.

Denavit, J., and R. S. Hartenberg. 1955. “A Kinematic Notation for Lower-Pair Mechanisms Based on Matrices.” Journal of Applied Mechanics 22 (2): 215–21. https://doi.org/10.1115/1.4011045.

Deng, Q., Bing Li, H.L. Huang, Rui Qing Liu, and Zong Quan Deng. 2010. “Design and Analysis of a Tapered Deployable Mast.” Key Engineering Materials 450 (November): 31–34. https://doi.org/10.4028/www.scientific.net/kem.450.31.

E. Ramirez. “Shuttle Radar Topography Mission.” NASA. Accessed June 18, 2022. https://www2.jpl.nasa.gov/srtm/mast_photos.html.

Galvez, Roberto, S. Gaylor, C. Young, N. Patrick, D. Johnson, and J. Ruiz. 2011. “The Space Shuttle and Its Operations.” NASA. 54-57.

Gardner, Jonathan P., John C. Mather, Mark Clampin, Rene Doyon, Matthew A. Greenhouse, Heidi B. Hammel, John B. Hutchings, et al. 2006. “The James Webb Space Telescope.” Space Science Reviews 123 (4): 485–606. https://doi.org/10.1007/s11214-006-8315-7.

Gross, Dave, and Dave Messner. 1999. “The Able deployable articulated mast - enabling technology for the Shuttle Radar Topography Mission.” In 33rd Aerospace Mechanisms Symposium, May 19-21, 1999. Pasadena, CA.

Hanaor, A., and R. Levy. 2001. “Evaluation of Deployable Structures for Space Enclosures.” International Journal of Space Structures 16 (4): 211–29. https://doi.org/10.1260/026635101760832172.

Hedgepeth, John M., and Louis R. Adams. 1986. “Rigid Diagonal Deployable Lattice Column.” U.S. Patent 4,569,176 issued February 11, 1986. https://patents.google.com/patent/US4569176A.

Jensen, F., and S. Pellegrino. 2001. “Arm Development Review of Existing Technologies.” Report No. CUED/D-STRUCT/TR-198. Department of Engineering, University of Cambridge, Cambridge, UK. http://www-civ.eng.cam.ac.uk/dsl/publications/TR198.pdf

Kim, Yunjin, Jason Willis, Suzanne Dodd, Fiona Harrison, Karl Forster, William Craig, Manfred Bester, and David Oberg. 2013. “Nuclear Spectroscopic Telescope Array (NuSTAR) Mission.” In 2013 IEEE Aerospace Conference, March 2-9, 2013, 1-9. Big Sky, MT: IEEE.

Kiper, Gökhan, Murat Demirel, Yunus Cebeci. 2019. “Katlanabilir Direk Yapısı.” Patent Application No: TR 2019 22860 A3.

Kiper, Gökhan and Eres Söylemez. 2009. “Deployable space structures.” In 2009 4th International conference on recent advances in space technologies, June 11-13, 2009, 131-138. Istanbul, Turkey: IEEE.

Kiper, Gökhan and Eres Söylemez. 2011. “Modified Wren platforms.” In 13th IFToMM world congress, June 19-23, 2011. Guanojuato, Mexico: Member Organization Mexico of IFToMM.

Kitamura, Takayuki, Koichi Yamashiro, Akira Obata, and Michihiro Natori. 1990. “Development of a High Stiffness Extendible and Retractable Mast ‘Himat’ for Space Applications.” 31st Structures, Structural Dynamics and Materials Conference, April 02-04, 1990. Long Beach, CA. https://doi.org/10.2514/6.1990-1054.

Kwan, A.S.K., Z. You, and S. Pellegrino. 1993. “Active and Passive Cable Elements in Deployable/Retractable Masts.” International Journal of Space Structures 8 (1-2): 29–40. https://doi.org/10.1177/0266351193008001-204.

Lee, Chung-Ching, and Jacques M. Hervé. 2014. “Bricard One-DoF Motion and Its Mechanical Generation.” Mechanism and Machine Theory 77 (July): 35–49. https://doi.org/10.1016/j.mechmachtheory.2014.02.004.

Mauch, Hagen R. 1967. “Deployable Lattice Column.” U.S. Patent 3,486,279 issued November 30, 1967. https://patents.google.com/patent/US3486279

John Michael Mccarthy, and Gim Song Soh. 2011. Geometric Design of Linkages. New York, NY: Springer.

McEachen, Michael. 2010. “Validation of SAILMAST technology and modeling by ground testing of a full-scale flight article.” 48th AIAA Aerospace Sciences Meeting Including the New Horizons Forum and Aerospace Exposition, January 04-07, 2010. Orlando, FL.

Mikulas, M. Martin Jr., and Mark Thomson. 1992. “LARGE SPACE STRUCTURES (State-of-The-Art and Technology Needs).” In 33rd Structures, Structural Dynamics and Materials Conference, April 13-16, 1992. Dallas, TX. https://doi.org/10.2514/6.1992-2448.

Murphey, Thomas W. 2006. Booms and Trusses. In Recent Advances in Gossamer Spacecraft, edited by Christopher H. M. Jenkins, 1-44. Reston, Virginia: American Institute of Aeronautics and Astronautics, Inc.

NASA. “Payload Fairing.” Accessed June 18, 2022. https://mars.nasa.gov/mer/mission/launch-vehicle/payload-fairing/.

Nataraju, B. S., and A. Vidyasagar. 1987. “Deployment dynamics of accordian type of deployable solar arrays considering flexibility of closed control loops.” In IAF, International Astronautical Congress, 38th, October 10-17, 1987. Brighton, England.

National Instruments. “MyRIO.” Accessed July 6, 2022. https://www.ni.com/en-tr/shop/hardware/products/myrio-student-embedded-device.html.

Pellegrino, S. 1995. “Large Retractable Appendages in Spacecraft.” Journal of Spacecraft and Rockets 32 (6): 1006–14. https://doi.org/10.2514/3.26722.

Puig, L., A. Barton, and N. Rando. 2010. “A Review on Large Deployable Structures for Astrophysics Missions.” Acta Astronautica 67 (1-2): 12–26. https://doi.org/10.1016/j.actaastro.2010.02.021.

Straubel, Marco. 2012. “Design and Sizing Method for Deployable Space Antennas.” Doctoral Thesis, Fakultät für Maschinenbau der Otto-von-Guericke-Universität Magdeburg. https://elib.dlr.de/81128/1/2013-02-08_Dissertation-Marco_Straubel-OnlineVersion.pdf.

Sun, Jianwei, Song Gao, Wenrui Liu, Fanchen Kong, and Xiaodong Li. 2022. “Design and Static Analysis of New Deployable Mechanisms Based on the Four-Bar Slider–Crank Mechanism.” Mechanics Based Design of Structures and Machines, 1–23. https://doi.org/10.1080/15397734.2022.2038617.

Tekno-Tel Yay. “Baskı Yayı” Accessed October 6, 2022. http://www.teknotelyay.com.tr/wp-content/uploads/2018/10/Katalog.pdf

The Spring Store. “Stock Torsion Springs Catalog” Accessed October 6, 2022. https://www.thespringstore.com/media/download-pdf-entire/Stock-Torsion-Spring-Catalog.pdf

Tibert, Gunnar. 2002. “Deployable Tensegrity Structures for Space Applications.” Doctoral Thesis, Royal Institute of Technology (KTH), Department of Mechanics. http://www-civ.eng.cam.ac.uk/dsl/publications/TibertDocThesis.pdf

Vorlicek, P. L., J. V. Gore, and C. T. Plescia. 1982. “Design and analysis considerations for deployment mechanisms in a space environment.” In 16th Aerospace Mechanisms Symposium, May 13-14, 1982. Kennedy Space Center, FL. https://ntrs.nasa.gov/api/citations/19820015484/downloads/19820015484.pdf

Wang, H., L. Zhao, H. Yu, Y. Zhao, and G. Chen. 2016. “Reconfigurable Extended Joint.” Patent no: CN104608117B issued May 25, 2016. https://patents.google.com/patent/CN104608117B

Wang, Jieyu, Xianwen Kong, and Jingjun Yu. 2022. “Design of Deployable Mechanisms Based on Wren Parallel Mechanism Units.” Journal of Mechanical Design 144 (6). https://doi.org/10.1115/1.4053282.

Warden, Robert M. 1987. "Folding, articulated, square truss." In 21st Aerospace Mechanisms Symposium, May 01, 1987. NASA-Lyndon B. Johnson Space Center, Houston, TX. https://ntrs.nasa.gov/api/citations/19870020426/downloads/19870020426.pdf

Wie, B., N. Furumoto, A. K. Banerjee, and P. M. Barba. 1986. “Modeling and Simulation of Spacecraft Solar Array Deployment.” Journal of Guidance, Control, and Dynamics 9 (5): 593–98. https://doi.org/10.2514/3.20151.

Xue, Nian-pu, Feng Ding, Biao Li, Qiong Wu, and Dong-jian Xie. 2018. “The Influence Parameters of 60m Able Deployable Articulated Mast Mode.” Proceedings of the International Symposium on Big Data and Artificial Intelligence, December 29-30, 2018. Hong Kong, Hong Kong. https://doi.org/10.1145/3305275.3305335.

Zhao, Longhai, Hao Wang, Genliang Chen, and Shunzhou Huang. 2018. “Sequentially Assembled Reconfigurable Extended Joints: Self-Lockable Deployable Structure.” Journal of Aerospace Engineering 31 (6). https://doi.org/10.1061/(asce)as.1943-5525.0000877.